DESIGNING AND PLANNING FOR SAFE PEDESTRIAN PATHS AT RAIL TRANSIT STATIONS SERVING RITI COMMUNITIES

FINAL PROJECT REPORT
By

Roger B. Chen[1], Xiazhi Zhang, Poya Harirchi, Marissa Chun

[1]Principle Investigator

Department of Civil, Environmental and Construction Engineering
University of Hawaii at Manoa

Center for Safety Equity in Transportation (CSET)
USDOT Tier 1 University Transportation Center
University of Alaska Fairbanks
ELIF Suite 240, 1764 Tanana Drive
Fairbanks, AK 99775-5910

rural · isolated · tribal · indigenous

DISCLAIMER

The contents of this report reflect the views of the authors, who are responsible for the facts and the accuracy of the information presented herein. This document is disseminated under the sponsorship of the U.S. Department of Transportation's University Transportation Centers Program, in the interest of information exchange. The Center for Safety Equity in Transportation, the U.S. Government and matching sponsor assume no liability for the contents or use thereof.

TECHNICAL REPORT DOCUMENTATION PAGE

1. Report No.	2. Government Accession No.	3. Recipient's Catalog No.

4. Title and Subtitle	5. Report Date
DESIGNING AND PLANNING FOR SAFE PEDESTRIAN PATHS AT RAIL TRANSIT STATIONS SERVING RITI COMMUNITIES	6/30/2024
	6. Performing Organization Code

7. Author(s) and Affiliations	8. Performing Organization Report No.
Roger B. Chen, Xiazhi Zhang, Poya Harirchi, Marissa Chun Department of Civil, Environmental and Construction Engineering	INE/CSET 24.12

9. Performing Organization Name and Address	10. Work Unit No. (TRAIS)
Center for Safety Equity in Transportation ELIF Building Room 240, 1760 Tanana Drive Fairbanks, AK 99775-5910	
	11. Contract or Grant No. 69A3551747129

12. Sponsoring Organization Name and Address	13. Type of Report and Period Covered
United States Department of Transportation Research and Innovative Technology Administration 1200 New Jersey Avenue, SE Washington, DC 20590	Final Report
	14. Sponsoring Agency Code

15. Supplementary Notes

Report uploaded to:

16. Abstract

In this study, we focus on pedestrian network construction and pedestrian route choice analysis. We developed a GIS based framework for pedestrian network construction, which takes multiple data sources, such as open source networks, satellite imagery, and pedestrian GPS traces. The pedestrian route choice study examines the impact from tradeoffs between environmental and infrastructure attributes, such as ambient noise, tree canopy shade, and surface characteristics (e.g., sidewalk, grass, etc.). We investigate these in a university campus setting, where walking trips comprise about 25% of all commute trips, with a greater percentage expected for within campus OD trips. We collect and analyze GPS data from volunteer community members of the University of Hawaii at Manoa (UHM), resulting in 298 distinct observed OD trips and their routes. From a RUM route choice standpoint, choice set generation is a difficult problem, especially for on-campus walking, which is unrestricted and can deviate from discrete roadways or sidewalks. Thus, a recursive logit route choice model is estimated to determine the tradeoffs between route link attributes, such as ambient noise, tree canopy shade, and other infrastructure attributes. The estimated recursive logit model and network construction framework were applied to four identified Skyline stations to analysis the pedestrian route choice behavior when accessing the stations.

17. Key Words		18. Distribution Statement	
Pedestrians, Walking, Route Choice, Network Analysis			
19. Security Classification (of this report)	**20. Security Classification (of this page)**	**21. No. of Pages**	**22. Price**
Unclassified.	Unclassified.	42	N/A

Form DOT F 1700.7 (8-72)   **Reproduction of completed page authorized.**

SI* (MODERN METRIC) CONVERSION FACTORS

APPROXIMATE CONVERSIONS TO SI UNITS

Symbol	When You Know	Multiply By	To Find	Symbol
LENGTH				
in	inches	25.4	millimeters	mm
ft	feet	0.305	meters	m
yd	yards	0.914	meters	m
mi	miles	1.61	kilometers	km
AREA				
in^2	square inches	645.2	square millimeters	mm^2
ft^2	square feet	0.093	square meters	m^2
yd^2	square yard	0.836	square meters	m^2
ac	acres	0.405	hectares	ha
mi^2	square miles	2.59	square kilometers	km^2
VOLUME				
fl oz	fluid ounces	29.57	milliliters	mL
gal	gallons	3.785	liters	L
ft^3	cubic feet	0.028	cubic meters	m^3
yd^3	cubic yards	0.765	cubic meters	m^3
NOTE: volumes greater than 1000 L shall be shown in m^3				
MASS				
oz	ounces	28.35	grams	g
lb	pounds	0.454	kilograms	kg
T	short tons (2000 lb)	0.907	megagrams (or "metric ton")	Mg (or "t")
TEMPERATURE (exact degrees)				
^{o}F	Fahrenheit	5 (F-32)/9 or (F-32)/1.8	Celsius	^{o}C
ILLUMINATION				
fc	foot-candles	10.76	lux	lx
fl	foot-Lamberts	3.426	candela/m^2	cd/m^2
FORCE and PRESSURE or STRESS				
lbf	poundforce	4.45	newtons	N
lbf/in^2	poundforce per square inch	6.89	kilopascals	kPa

APPROXIMATE CONVERSIONS FROM SI UNITS

Symbol	When You Know	Multiply By	To Find	Symbol
LENGTH				
mm	millimeters	0.039	inches	in
m	meters	3.28	feet	ft
m	meters	1.09	yards	yd
km	kilometers	0.621	miles	mi
AREA				
mm^2	square millimeters	0.0016	square inches	in^2
m^2	square meters	10.764	square feet	ft^2
m^2	square meters	1.195	square yards	yd^2
ha	hectares	2.47	acres	ac
km^2	square kilometers	0.386	square miles	mi^2
VOLUME				
mL	milliliters	0.034	fluid ounces	fl oz
L	liters	0.264	gallons	gal
m^3	cubic meters	35.314	cubic feet	ft^3
m^3	cubic meters	1.307	cubic yards	yd^3
MASS				
g	grams	0.035	ounces	oz
kg	kilograms	2.202	pounds	lb
Mg (or "t")	megagrams (or "metric ton")	1.103	short tons (2000 lb)	T
TEMPERATURE (exact degrees)				
^{o}C	Celsius	1.8C+32	Fahrenheit	^{o}F
ILLUMINATION				
lx	lux	0.0929	foot-candles	fc
cd/m^2	candela/m^2	0.2919	foot-Lamberts	fl
FORCE and PRESSURE or STRESS				
N	newtons	0.225	poundforce	lbf
kPa	kilopascals	0.145	poundforce per square inch	lbf/in^2

*SI is the symbol for the International System of Units. Appropriate rounding should be made to comply with Section 4 of ASTM E380.
(Revised March 2003)

Table of Contents

List of Figures

List of Tables

EXECUTIVE SUMMARY

In 2023, the first segment of the Skyline Rail System in Honolulu, Hawaii (Kualaka'i East Kapolei Station to Aloha Stadium Station) officially went into service. This rail system represents a significant investment in urban transportation infrastructure aimed at alleviating traffic congestion and enhancing mobility on the island of Oahu. Skyline stations face forecasted ridership that predominantly lives in West Oahu, such as East Kapolei and Waipahu, where RITI (rural isolated tribal and indigenous) passengers have higher percentages relative to the Honolulu urban core. Additionally, the combination of high passenger volumes and location of stations next to highway facilities may require the construction of a grade separation structure for pedestrians.

In this project we developed a framework and approach for estimating pedestrian flow rates at transit stations. This framework supports the design and planning of pedestrian paths surrounding transit stops in heavily congested areas with high volumes of vehicle traffic. Jurisdictions deciding among infrastructure investments can benefit from understanding the tradeoffs between route attributes that pedestrians face, especially those related to the environment and infrastructure, such as providing a sidewalk versus an open grass area or more tree shading.

To construct and test our proposed framework, we conducted an experiment on pedestrian route choice at the campus of the University of Hawaii at Manoa, where walking is a predominant mode of transportation. We developed a GIS based framework for pedestrian network construction, which takes multiple data sources, such as open source networks (e.g., OSM), satellite imagery, and pedestrian GPS traces. The pedestrian route choice study examines the impact from tradeoffs between environmental and infrastructure attributes, such as ambient noise, tree canopy shade, and surface characteristics (e.g., sidewalk, grass, etc.). We collected and analyzed GPS data from volunteer community members of the University, resulting in 298 distinct observed origin-destination (OD) trips and their routes.

From a random utility model (RUM) route choice standpoint, choice set generation is a difficult problem, especially for on-campus walking which is unrestricted and can deviate from discrete roadways or sidewalks. Thus, a recursive logit route choice model is estimated to determine the tradeoffs between route link attributes, such as ambient noise, tree canopy shade, and other infrastructure attributes. The recursive logit model is a link-based model, which formulates the route choice problem as link choice problem at each node. The estimated recursive logit model and network construction framework were then applied to four identified Skyline stations to analysis the pedestrian route choice behavior when accessing the stations. The estimation results indicate that sidewalks, grass surfaces, and a tree canopy are preferred over links that traverse quadrangles. Pedestrians have a higher likelihood of choosing a route with more sidewalks, grass surface and less sun exposure. With respect to noise, traversing quadrangles and parking lots is preferable than sidewalks, grass surface, and tree canopy.

Finally, an individual pedestrian network was constructed for each identified Skyline station to cover the point of interests in walking distance. Ten OD pairs were selected for pedestrian flow distribution analysis at each station. We applied our final model specification to calculate the pedestrian flow distribution on the network. We found that as pedestrian traffic needs to cross major highways to access the Skyline stations at Waiawa Pearl Highlands, Kualaka'i East Kapolei, and Keone'ae U.H. West Oahu,

and given that the Skyline ridership is expected to increase in the future, this issue might become a major risk to pedestrian safety.

CHAPTER 1. INTRODUCTION

Providing sustainable options to travelers continues to motivate discussion on prioritizing infrastructure investments for active travel modes at all jurisdiction levels, from cities to the US states. The City and County of Honolulu (CCH) and the Hawaii Department of Transportation (HDOT) have developed and adopted pedestrian master plans, with similar efforts in other US jurisdictions (CCH Department of Transportation Services, 2022; Hawaii Department of Transportation, 2013). Walking as a travel mode is a low-cost, accessible, and sustainable way to travel short distances, particularly within dense urban areas and campuses with limited vehicle access. Additionally, walking, as an active travel mode, is associated with improvements in physical and mental health compared to passive modes, like driving and public transit (Singleton, 2019). For the UH-Manoa (UHM) campus, walking accounts for 25% percent of commute trips to campus, according to their *Campus Travel Demand Management Plan* (University of Hawai'i at Manoa, 2012). In the Waikiki Special District, walking accounts for 56% percent of visitor trips (CCH Department of Transportation Services, 2022; Hawaii Department of Transportation, 2013). Jurisdictions deciding among infrastructure investments can benefit from understanding the tradeoffs between route attributes that pedestrians face, especially those related to the environment and infrastructure, such as providing a sidewalk versus an open grassy area or more tree shading. A route choice analysis for major origin-destination (OD) pairs in a network can also help prioritize attributes relevant in a pedestrian's route choice process and support design decisions. These require forecasting tools for making well-informed, consistent assessments of future conditions under various scenarios, specifically the relationship between the routes pedestrians choose and other network attributes. Behavioral models are at the heart of these tools. Methodologically, this requires models to better understand and forecast different behavioral rationales in response to attributes faced by pedestrians, such as noise level, tree shade, and infrastructure topography.

In 2023, the first segment of the Skyline Rail system (Kualaka'i East Kapolei Station to Aloha Stadium Station) was officially in service. This project represents a significant investment in urban transportation infrastructure aimed at alleviating traffic congestion and enhancing mobility on the island of Oahu. Skyline stations face forecasted ridership that predominantly lives in West Oahu, such as East Kapolei and Waipahu, where RITI (rural isolated tribal and indigenous) passengers have higher percentages relative to the Honolulu urban core. Additionally, the combination of high passenger volumes and location of stations next to highway facilities may require the construction of a grade separation structure for pedestrians. For example, the Waiawa Station may need high-capacity crossover access for large volumes of passengers that need to cross the Kamehameha Highway to reach the Pearl Highlands Shopping Center. The Federal Railroad Administration (FRA) recommends that railroads with busy passenger stations located on multi-track rail lines with frequent freight service should investigate the application of a high-capacity grade separation structure to carry large volumes of pedestrians.

In this project, we developed a framework and approach for estimating pedestrian flows distribution at identified Skyline transit stations. To construct and test this framework, we conducted an experiment on pedestrian route choice at the campus of The University of Hawaii at Manoa (UHM), where walking is a predominant mode of transportation in this area. This project makes three contributions.

(i) First, we present a method for generating and updating an underlying pedestrian network from GPS traces. As an illustrative case, we collect and analyze GPS traces from volunteer community members at UHM, resulting in 298 observed routes across the UHM campus and its surrounding neighborhood.

(ii) Second, we model pedestrian route choice with a recursive logit, avoiding the need for choice set generation, and analyze the effect of multiple attributes on pedestrians' route choice behavior. This is a specific advantage since pedestrian networks are complex due to a wider range of movement across spaces, such as open plazas and grass areas.

(iii) Third, we apply our findings at identified Skyline transit stations. Detailed pedestrian network is developed at each identified station. We calculate pedestrian flow distribution for pedestrian traffic accessing the stations with our calibrated recursive logit model.

The remainder of this report is structured as follows. In section 2, we present previous works in this field. In section 3, we discuss the experiment conducted at UHM, this includes GPS trace collection and processing, the study area, and the network generation including link attributes. This is followed by a presentation on the recursive logit. In section 4, we present and discuss the estimation results from the recursive logit model for pedestrian route choice. In section 5, we present the pedestrian flow distribution analysis at identified Skyline transit stations. Finally, in Section 6, we provide our concluding remarks.

CHAPTER 2. REVIEW OF LITERATURE

2.1 Pedestrian Route Choice

Past mode choice studies indicate that walkability which measures *walk friendliness* is important in pedestrian route choice. Additionally, environments with walkability positively influence destination choices, pedestrians tend to choose destinations with better pedestrian environments (Clifton et al., 2016). The literature indicates that pedestrians tend to choose paths that are safe (Amoh-Gyimah et al., 2016), comfortable, and pleasant to walk on (Guo, 2009; Ryan and Frank, 2009; Tal and Handy, 2012). One important dimension of walkability is environmental quality, which has been measured with roadway and/or infrastructure attributes, in addition to environmental conditions, such as noise, sunlight and other qualitative factors. Previous studies agree on common factors, such as distance, amenities (e.g., side places to sit/rest), sidewalk width, sunlight exposure, noise exposure, street network connectivity, number of turns and crossings, crossing types, etc. (Bovy and Stern, 2012; Guo and Loo, 2013; Sevtsuk et al., 2021; Singleton et al., 2021; Tal and Handy, 2012). However, these studies do not provide insights into the tradeoffs among these factors, which can support infrastructure investment decisions that face a fixed money budget.

Because of its human-scale, pedestrian walking experiences are shaped by attributes differently from drivers, emphasizing those relating to personal exposure. Previous studies consistently show that besides minimizing travel time and distance, other built/natural environment and land use characteristics also statistically explain route choices that deviate from the shortest path (Guo and Loo, 2013; Lue and Miller, 2019; Sevtsuk et al., 2021). Studies indicate that noise levels negatively impact pedestrian route choices, with pedestrians avoiding noisy routes, in general (Base et al., 2022; Basu and Sevtsuk, 2022; Bovy and Stern, 2012). Guo and Loo (2013) conducted studies in Hong Kong and New York City, which identified noise as an explanatory factor for comfort in pedestrian route choice (Guo and Loo, 2013). de Jong and Fyhri (2023) conducted a geospatial survey using the Google Maps API, revealing that noise contributes to an adverse experience for cyclist in urban networks, potentially leading to sensory overload; a similar impact on pedestrians is expected. Wang et al. (2020) proposed a network routing model which integrates traffic noise; this model aims to minimize noise exposure along generated routes. They developed a traffic estimation model that incorporates multiple datasets to estimate the network traffic volumes. Using a modified version of Dijkstra's shortest path algorithm, they generated routes constrained by both distance and noise exposure (Wang et al., 2020).

Current approaches to route choice analysis using random utility model (RUM) discrete choice models are roughly categorized as either *path-based* or *link-based* approaches. In previous studies, path-based models were more conventional, but face significant barriers (Prashker and Bekhor, 2004; Vovsha and Bekhor, 1998; Zimmermann et al., 2017). In dense urban areas, a complex network can have an unlimited number of paths connecting a single OD pair, if loops are allowed (Bekhor, 2006; Ghanayim and Bekhor, 2018; Prashker and Bekhor, 2004; Zimmermann et al., 2017). For route choice model estimation, a choice set for each OD pair needs to be defined (Zimmermann et al., 2017). This leads to a well-known challenge associated with path-based models called the *route choice set generation problem* (Ramming, 2001). There are several methods commonly used for choice set generation, such as *K-*

shortest paths (Eppstein, 1998), *route labeling* (Ben-Akiva et al., 1984), *link elimination* (Azevedo et al., 1993)*, link penalty* (Barra et al., 1993)*,* and *data driven methods* (Yao and Bekhor, 2020)*.* The *K-shortest path* method finds a given number (*K*) of paths that are longer than the shortest path for a given OD pair (Bekhor et al., 2006; Eppstein, 1998)*.* The *route labeling approach* exploits the availability of path attributes to formulate different functions that produce alternative routes. These routes may be labeled according to criteria such as "minimize distance," "minimize turns" or "maximize use of expressways" (Bekhor et al., 2006; Ben-Akiva et al., 1984)*.* The *link elimination method* removes links at each iteration and finds the new shortest path after link removal (Azevedo, 1993; Sevtsuk et al., 2021). In recent years, machine learning-based approaches such as clustering, random forests (Yao and Bekhor, 2020), decision trees (Ciscal-Terry et al., 2016), multiple types of neural networks (Lai et al., 2019; Sun and Park, 2017), and autoencoders (Yao and Bekhor, 2022) have also been used for choice set generation*.* An alternative to path-based approaches is a link-based recursive approach, discussed later in Section 2.

2.2 Pedestrian Network Modeling

Past studies focusing on pedestrian networks are extremely rare relative to other active travel modes, such as transit and cycling (Broach et al., 2012; Casello and Usyukov, 2014; Raveau et al., 2011)*.* These studies fall under two broad categories: (a) studies focused on generating the underlying physical network and (b) studies focused on flow dynamics and congestion. Unlike motorized traffic, pedestrians can move freely through lawns, parking lots, buildings, open plazas etc. Using a conventional discrete network representation, such as networks from OpenStreetMap, to approximate pedestrian traffic may be unsatisfactory. Methods for generating a precise underlying network are roughly categorized as: (a) manual digitization; (b) aerial image processing; and (c) crowdsourced mapping. Hu et al*.* (2007) developed an aerial image-based two-step automatic road network extraction method. Their method shows promise in extracting networks that follow the *observed roads*, but face limitations for extracting off-road paths. Kasemsuppakom and Karimi (2013) developed a method to construct pedestrian network from multiple GPS traces. They use the geometric properties of GPS points for filtering and merging traces. Zhou et al. (2020) developed an approach for pedestrian network construction based on crowdsourced walking trajectories. They convert GPS traces into density maps, where a high density was considered a walkway, similar to the process in this study.

Pedestrian flows have received moderate attention in the transportation systems literature. Daamen et al. (2002) and Hoogendoorn and Bovy (2004, 2005) both focused on pedestrian flow in transit stations. Their model dynamically incorporates real-time data to optimize station layout and timetable design to improve flow efficiency. Hoogendoorn et al. (2015) developed a multi-class continuum model to address pedestrian flow dynamics. Their model differentiated between global and local route choices, capturing pedestrian self-organization, such as lane and diagonal stripe formation. Saberi et al. (2015) used empirical data to study pedestrian behavior in bidirectional streams. They show that self-organization strongly influences the velocity distribution and for the same crowd size, and that velocity distributions are similar regardless of whether pedestrians are mixed or in separated lanes. Shahhoseini et al. (2018) used empirical data and simulation models to analyze the interactions and adaptations of pedestrians as they merge from different streams. They conclude that increased density at merger points can lead to reduced speeds and increased travel times.

6

Zhang et al. (2021) developed a framework for designing pedestrian guideways that improve traffic efficiency and safety under congested overcrowded conditions. They use a set of nonlinear partial differential equations to describe pedestrian route choice under a Nash Equilibrium and present numerical examples to show its effectiveness. Feliciani and Nishinari (2018) developed a trajectory-based method for measuring pedestrian crowd levels based on the velocity field around a region of interest. In their experiment, the experimental area was divided into small cells, and a velocity vector field was obtained from the pedestrian trajectory data. Their method was able to detect congestion in a periodic bidirectional stream where density and flow did not vary significantly, and which could not be studied in detail using the fundamental diagram. Zanlungo et al. (2023) developed a simpler approach named the Congestion Number based on the differentials of velocity field. Their experiment showed that the Congestion Number can be applied to various settings, such as bottlenecks and places with multi-directional flows.

2.3 Synthesis and Summary:

A literature review on pedestrian route choice indicates that several factors relating to the infrastructure and perceived environment affect choices. However, few studies attempt to estimate the tradeoffs among these factors estimated from actual route choice data. From the standpoint of investing in infrastructure, understanding these tradeoffs helps determine the return on investment for different designs and facilities, relative to other factors. For example, understanding tradeoffs between noise levels on a paved walkway versus other walkway types allows prioritizing for minimizing the negative impact from ambient noise. In this project we examined pedestrian route choices and the tradeoffs they make with respect to network link attributes, such as shade coverage from tree canopies and the infrastructure topography, with the end goal of informing investment decisions.

CHAPTER 3. METHODOLOGY AND MODEL CONSTRUCTION

This section discusses the pedestrian route choice study conducted at the UHM campus. This includes data collection and processing, and the recursive logit approach to route choice modeling. The overall analysis framework is presented in Figure 1. The framework begins with collecting actual route choice data and updating an initial network graph representing pedestrian travel with these data. In this case, OpenStreetMap (OSM) was used to provide an initial network graph. Given an updated network graph, we perform map matching between the observed routes and the updated network to generate a route choice data set for further analysis.

3.1 Study Area:

A map of the study area is provided in Figure 2 and was determined based on multiple factors, including the official university campus boundary and feasible walking distances to this boundary. For the University of Hawaii at-Manoa (UHM) campus, walking accounts for 25% percent of commute trips to/from campus (University of Hawai'i at Manoa, 2012). Empirically and anecdotally, we observed pedestrians taking paths at multiple locations where those paths are not covered in the initial OSM network graph. Also shown in Figure 2 is a density plot over the collected GPS trace data, with darker red areas indicating a higher concentration and yellow areas indicating lower concentration of traces. In specific sections of the study area, the sidewalk network does not align with the heavy walking traffic areas.

Community GPS Trace Data

Person 1 Person 2 Person n

Network Updating Process

Community Contributions (**GPS Points, Drawings, Health Trackers –** *Strava/Garmin/Fitbit***, etc.**) +

Other Data (**OSM, etc**.)

Other Data Sources

OpenStreetMap

Sidewalk Map (Walking Audit)

Updated Network

Traveler **Routes (Paths)** and **Networks**: Behavioral Modeling

Personal Networks

Personal Routes

Scenario Analysis: **Network Modeling and Traffic Analysis**

- Infrastructure Projects
- Operational Improvements
- Community Evacuations
- Planned Traffic Disruptions
- Other Scenarios

Figure 1. Analysis Framework

9
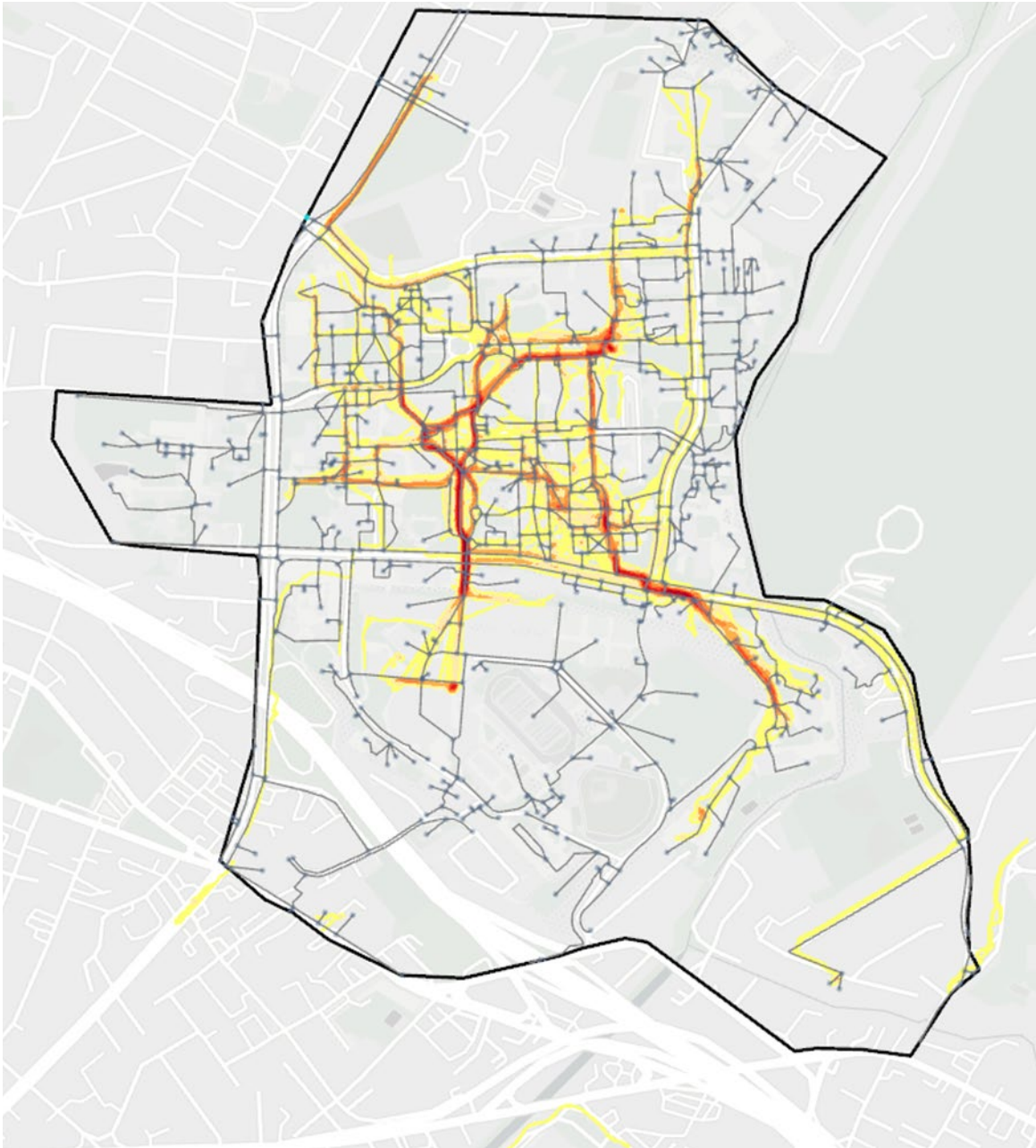
Figure 2. University Campus Study Area and Collected GPS Trace Data Densities

3.2 GPS Trace Data Collection and Processing for Route Choice Modeling

This section presents the process for collecting GPS trace data from study participants and the subsequent data processing for generating a route choice dataset. These data were integrated with a publicly available network graph, in this case from OpenStreetMap (OSM), to generate an *updated* pedestrian network graph that was attributed for subsequent analysis and model estimation.

3.2.1 GPS Data Collection

Personal GPS data collection was initiated with 55 community volunteers drawn from the College of Engineering. However, due to participant attrition and data logging errors, only GPS trace data from 16 volunteers were retrained for analysis. Recruitment was accomplished through student organization and staff email listservs. Data collection occurred only on weekdays for a two-week period in April 2023. During this period, participants started logging GPS data daily, when they first left their homes and stopped when they returned home without returning to campus for the remainder of the day. GPS points were logged in two second intervals. Participants were asked to install a free GPS data logging app on their smartphones to accomplish this, either *UltraGPSLogger* for Android or *TripLogger Remote* for iOS.

3.2.2. GPS Data Processing

After collecting the data, processing the GPS traces occurs in three main steps that work towards removing points that have unacceptable measurement errors or are irrelevant to route choice. Additionally, once a pedestrian network is generated, route choice data is generated by matching observed GPS traces with the network, outputting an actual route in our graph network.

Step 1 – Remove GPS points with Intolerable Measurement Errors and Irrelevant to Route Choice: The first step requires removing a subset of GPS points for one of two reasons: (a) they were logged with potential receiving errors or (b) they clustered within a building and were irrelevant for route choice analysis. However, GPS points that are part of routes that traverse through a building were retrained. Measurement errors for GPS points occur for several reasons, including interference from clouds/buildings/windows and insufficient satellites within range to triangulate a position (Merry and Bettinger, 2019). Points were filtered for potential receiving errors based on the *horizontal dilution of precision (HDOP)*, GPS points with HDOP value greater than 15 were filtered (Kasemsuppakorn and Karimi, 2013). HDOP reflects the geometric strength of the configuration of satellites relative to a receiver, which quantifies the level of accuracy in horizontal position readings (Langley, 1999). To remove building interior points (that were not part of a traversing route), a shapefile of building boundaries, from UH Facilities, was used in GIS to remove points falling inside the boundaries within a two-meter buffer, but not clustered (which would indicate an activity). These were considered indoor points and removed.

Step 2 – Distinguishing between Travel and Activity: To distinguish between points comprising travel from other activities, the method based on spatial point density from Schüssler and Axhausen, (2008) was adopted. When the participant is relatively stationary, indicating an activity, the GPS points will cluster closely within a small area, leading to a high density (Schüssler and Axhausen, 2008). For each GPS point, the point density is calculated by determining how many of the 30 preceding and succeeding GPS points, based on timestamps, are within a 15-meter radius of the point of interest (Schüssler and Axhausen, 2008). If the density is greater than 15 points with a 15-meter radius circular area, for at least 3 minutes, then an activity is detected. If two detected activities are close spatially to each other, and the time gap between them is less than 2 minutes, then the activities are merged. Finally, if the time gap between two consecutive points is greater than 5 minutes, then the trajectory is separated into two trips.

Step 3 – Distinguishing between Walking and Non-Waking Trips: The final step labels trip segments with a travel mode, specifically walking versus other (non-walking) modes. A neural network model was developed for this purpose. This neural network was developed as a binary classification model, the classification output was either pedestrian or non-pedestrian. Identifying the exact GPS (single) point where travel mode changes is difficult because of short recording intervals and natural errors of GPS recording. Additionally, an individual generally would not change mode very frequently. Hence, the trip data was divided into continuous small pieces, each piece contains roughly 20 seconds of data. Attributes used to classify trip segments were average speed, standard deviation of speed, maximum speed, and standard deviation of acceleration for each divided data piece (Byon et al., 2009; Yang et al., 2015). Each piece would be identified as either pedestrian or non-pedestrian. A sliding window algorithm was applied to identify the mode change location. If a mode change is identified, then input trip data is separated there to account for different modes. At this stage, all pedestrian trips have been identified from the GPS trace data.

Figure 3 illustrates these data processing steps. Figure 3a shows raw GPS trace data from a participant. Examples of clusters of points falling within buildings and those with potential receiving errors are indicated. Figure 3b illustrates the results from *Step 1*, where points are removed based on unacceptable HDOP values or because they fell within buildings. Figure 3c shows Step 2 which segments points into travel and activities. Figure 3d shows Step 3, where travel segments are classified into walk and non-walk modes by the neural network.
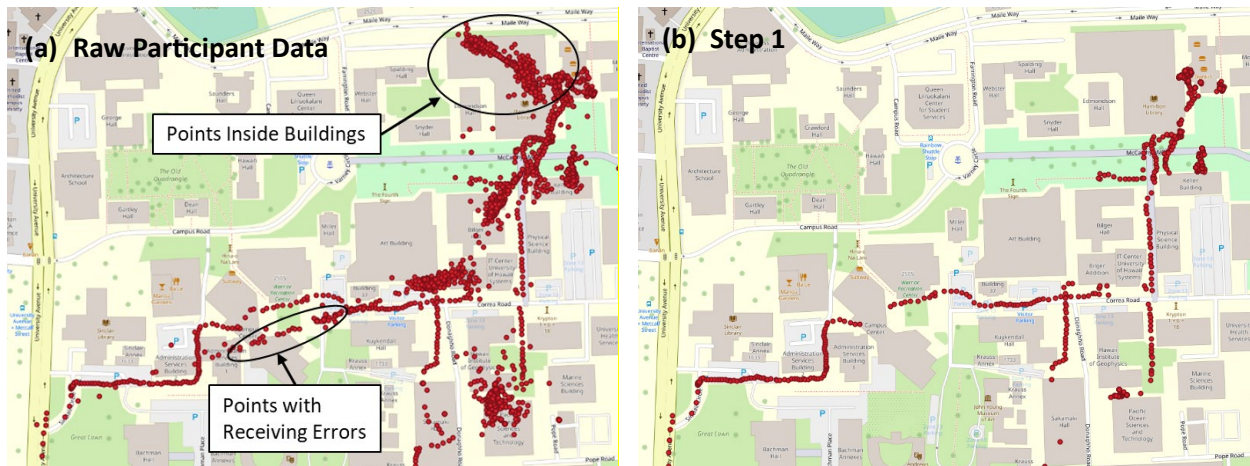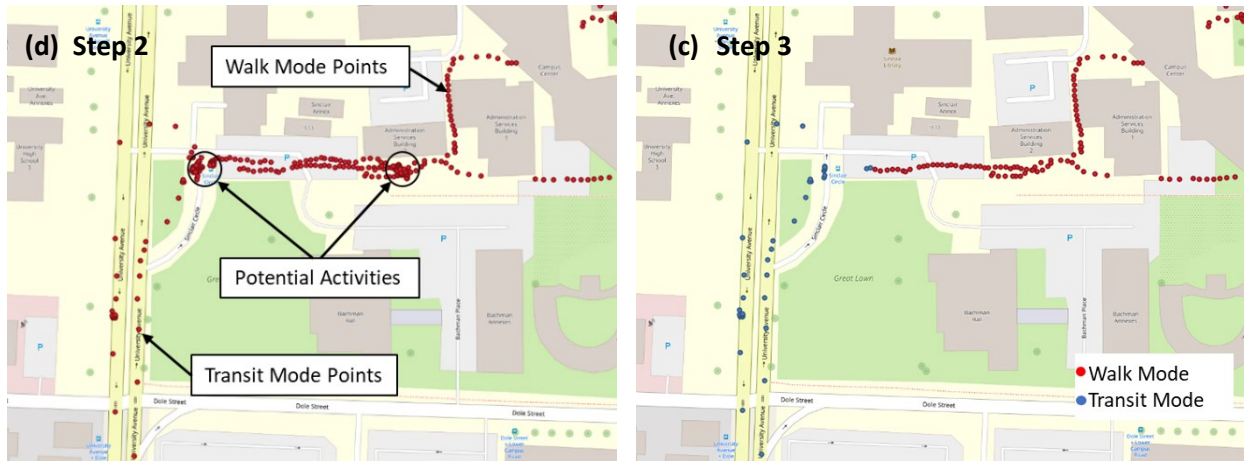
Figure 3. GPS Data Processing (a) Example of raw GPS data; (b) Step 1: HDOP and building point filtering; (c) Step 2: travel and activity segmentation; (d) Step 3: walking and non-walking segment classification

3.3 Network Generation and Matching

The network generation and map matching processes were conducted in a GIS environment. The purpose of these procedures is twofold. First, we wish to generate a pedestrian network graph (links and nodes) with link attributes (e.g., sidewalk links) that represent the space over which pedestrians move. Second, given this network, we match observed time-stamped GPS point data with the updated network to produce observed routes between OD pairs from our sample. The process begins with an initial "base" network from OpenStreetMap (OSM). The OSM network is incomplete and inaccurate, missing several segments that were traversed in the observed routes. This shortcoming has been documented in the literature (Lu and Zhou, 2023). Table 1 presents this process in greater detail.

Table 1: Network Generation and Matching Process

Main Steps	Example Image
0. Obtain Initial Pedestrian Path Shapefile – The network generation process begins with obtaining an existing path shapefile, which may be insufficient for pedestrian analysis due to missing links used commonly for walking. For this study an appropriate existing shapefile (or geospatial data source) was unavailable from the **City/County of Honolulu (CCH). Additionally, the shapefile** from OpenStreetMap (OSM) **was incomplete/inaccurate for the study area (Lu and Zhou, 2023). Thus, the authors manually created a shapefile of existing sidewalks in the study area, shown to the right with blue paths indicating sidewalks only.**	

1. **Augment with Observed Paths from GPS Trace Data** – Next, we augment the initial shapefile with the collected GPS trace data, which may traverse areas beyond sidewalks or initial coverage. GPS traces were clipped with a five-meter buffer around the existing path shapefile to account for inherent error in smartphone collected GPS data. The image to the right shows the initial path shapefile (blue) augmented **with clipped GPS traces from study participants** (red)**; many traversed the parking lot** (gray)**.**

2. **Estimate Line Density** – Given an augmented **path shapefile,** we estimate a density over the clipped GPS trace data to determine segments with significant traffic. For this paper, the line density was estimated within ArcGIS using the following parameters to create the raster: (a) pixel size of one meter; (b) search radius of five meters. **In the image to the left** a density is shown for the previous GPS traces used for augmentation; darker areas indicate higher observed traffic.
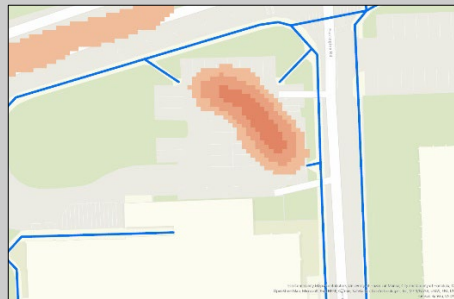
3. **Raster to Polygon Conversion** – In order to determine the location of links for augmenting the initial path shapefile, a threshold for a "significant" density value was assumed and used to obtain a polygon or area of the density meeting this threshold. For this paper, we used "**Jenks natural breaks classification," which clusters data into groups to minimize variance within groups and maximize the variance between them (Chen et al. 2013; Delso et al., 2017). The raster data was classified into two classes using the Jenks method to distinguish between higher and lower traversed areas. The resulting reclassified raster data was converted to polygons.**

4. **Augmenting Path Creation and Network Updating** – Centerlines which represent high pedestrian activity areas not covered in the existing network were created by drawing a centerline through the polygons from Step 3. The image to the right shows the centerline (black) from the polygon from Step 3. This represents areas of high pedestrian traffic not captured by the initial path shapefile.

5. **Conversion to a Graph (Links and Nodes)** -In this step, the created paths shapefile from Step 4 was converted to a graph of links and nodes, which serves as the representation of a network for this paper. The shapefile was first assessed for topology errors, such as lines that intersect with themselves. The resulting graph includes edges representing links (light blue) **for pedestrian travel and nodes** (dark blue) **connecting the links where travel from one edge to another** is possible**.**	
6. **Network (Map) Matching** – Given the graph which serves as our network topology, the final step _matches_ observed GPS traces consisting of points with the graph shapefile from Step 5 to determine observed paths. This was performed using the ArcGIS Network Analysis tool. The shortest route between an OD pair with intermediate points from the participant are calculated and exported as shapefiles for each trip; this is the observed route for the participant for a specific OD.	

3.4 Determining Link Attributes

As described in Step 5 of Table 1 above, links were created from the conversion of the paths shapefile to a graph of links and nodes. For further pedestrian route choice modeling, links need to be attributed beyond distance. The link attributes used in this study and corresponding generation methods are as follows:

a) _Length_: The length of each link in the network was measured and determined in GIS;
b) _Paved Sidewalk_: Determined with a walking audit and satellite imagery from Google Maps;
c) _Gradient/Slope_: Determined by dividing the difference in elevation of the nodes at either link end, based on the U.S. Geological Survey (USGS) 10m DEM data;
d) _Tree Canopy_: For the Island of Oahu, tree canopy data is provided through a partnership between EarthDefine LLC, US Forest Service, National Oceanic and Atmospheric Administration (NOAA), and Hawaii Division of Forestry and Wildlife (EarthDefine LLC, 2021). The raster data for tree canopy were converted to a polygon shapefile for analysis;
e) _Traversing Parking Lots, Grass_, and _Quadrangles_: Determined with a walking audit. We define a _quadrangle_ as a space or a courtyard, usually rectangular in plan, the sides of which are entirely or mainly occupied by parts buildings (Fleming et al., 1980)_;_ and
f) _Noise Level:_ The noise data collection and interpretation process are discussed in detail in the next section.

Links were attributed as binary indicator variables based on the percentage of the link possessing the attribute of interest. For example, a link was labeled as "tree canopy" (with the binary variable taking a value of one) if 50% or more of a link was covered by a tree canopy.

3.5 Noise Data Collection and Processing

Noise Data Collection: 39 noise data collection locations were used to cover the campus study area using a grid system (Figure 4). The noise level for each location was measured six times per day (7:30, 9:30, 11:30, 13:30, 15:30, 17:30) for weekdays using a *Tadeto SL 720 Digital Sound Level Meter* sound measurement device. This device has a recording capability ranging from 30 dB to 135 dB, and an accuracy of +/-2 dB and a sampling rate of 0.125 seconds. The noise data was collected during the Fall 2023 semester. Although the noise measurements were collected after the GPS data collection study completed, both were collected during the regular semesters. We assume these noise conditions are consistent across these two time periods.

Noise Data Processing: A GIS-based workflow was developed to interpolate the point-based noise measurement into a raster surface that permits attributing links. The Kriging method was used to interpolate point noise measurements to a spatial distribution. This method assumes the distance between sample points reflects a spatial correlation; it is appropriate when there is a known spatially correlated distance or directional bias in the data (Oliver and Webster, 1990). Aumond et al. (2018) conducted a sound measurement experiment in Paris and demonstrated that the Kriging is a promising method to create sound maps. Gundogdu and Guney (2007) employed universal Kriging to perform spatial analysis of groundwater levels; Wu and Li (2013) used Kriging to interpolate the air temperature in the US. After applying Kriging, the noise distribution was segmented into multiple noise levels, each with a 5 dB increment. Noise level segments were assigned to the links. If a link is completely within the boundary of a certain noise category, then this noise level is assigned to the link. If a link traverses two noise categories, the noise level for this link is determined by computing a weighted average, where the weights correspond to the proportion of distance the link traverses each noise category. Figure 4 shows the interpretation boundary and a noise distribution for a Wednesday morning period. The average noise level for the morning period is 63.66 dB, while the average noise level for the afternoon period is 62.41 dB.
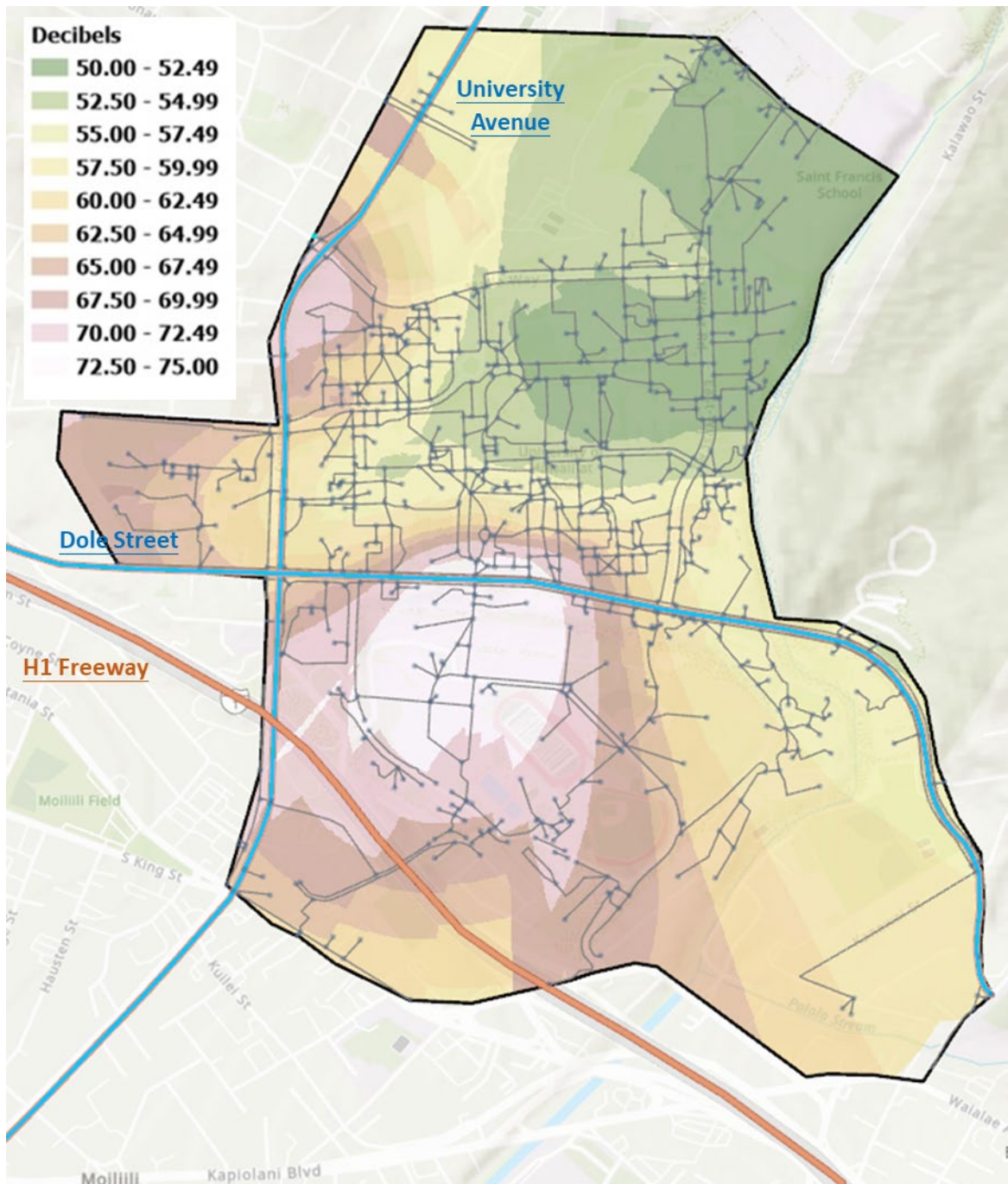
Figure 4. Noise Interpolation over the Study Area

3.6 Network and Route Attributes

The final updated network has 1,354 links and 1,084 nodes. The total distance for the network is 61,851 meters. Multiple link attributes were assigned: (a) link length; (b) link average grade; (c) sidewalk; (d) grass; (e) quadrangle; (f) tree canopy; (g) parking lot; and (e) noise level. Table 2 summarizes the network attributes. GPS traces from 55 volunteer community members were collected for a two-week period in April 2023. After processing the data, we only retained data from 16 participants with

acceptable GPS data quality and logging consistency. The final analysis sample consists of 298 trip OD pairs and routes. There are 67 unique OD pairs. The longest observed route was 1,791 meters, while the shortest observed route is 80 meters. The average observed route distance is about 532 meters. A summary of the observed route statistics was presented in Table 3. Only about 23.5% of the observed routes are similar within a tolerance to the shortest routes, which implies that in addition to distance, other attributes also play an important role in pedestrians route choice.

Table 2: Network Characteristics

Network Attributes		Percentage of Network Distance by Attribute	
Number of Links	1,354	Paved Sidewalk	79.3%
Number of Nodes	1,084	Grassy Surface	1.9%
Total Distance (meters)	61,851	Quadrangle	17.3%
Min Spanning Tree (meters)	39,395	Tree Canopy	5.1%
		Parking Lot	1.1%

Table 3: Observed Route Characteristics of ODs

Route Attributes	Observed Routes of ODs	Shortest Route of ODs
Number of Trips (Routes)	298	
Average Distance (meters)	532	474
Longest Distance (meters)	1,791	1,505
Shortest Distance (meters)	80	80
Average Percentage of Route (Distance-Based) across ODs		
Sidewalk	74.5%	69.7%
Grass Surface	2.1%	2.1%
Quadrangle	22.2%	23.7%
Tree Canopy	17.8%	16.8%
Parking Lot	1.6%	1.0%

3.7 Recursive Logit Model Formulation

In this section we present the formulation for the recursive logit (RL), a class of recursive models that has emerged in the recent route choice literature (Zhang et al. 2021). For a more detailed presentation, please see Fosgerau et al. (2013) and Zimmerman and Frejinger (2020). Previously, the majority of route choice modeling has been path (or route) based under a RUM framework, where the traveler chooses a route from a choice set of alternatives that maximizes his perceived utility; this requires specifying a route choice set, which is difficult depending on the network topology. The pedestrian network can be formulated as a directed connect graph $G = (A, V)$, where A is the set of links and V is the set of nodes.

In contrast to the path-based RUM framework, the recursive logit is formulated based on the framework of *Markov Decision Process* (MDP) used to solve stochastic shortest path problems in a dynamic programming context. In recursive models, network links correspond to *states*, while the outgoing links

from head node of the current link are available *actions* (Zimmerman and Frejinger, 2020). We will denote states as *k*, actions as *a,* and the deterministic utility of an action pair is $v(a|k)$, like previous studies (Fosgerau et al., 2013; Zimmerman and Frejinger, 2020; Zimmermann et al., 2017). The destination is represented by a dummy link *d*, which is an *absorbing state* of the MDP, where no additional utility is gained. A route under this framework is a sequence of states $\{k_0, k_1, k_2, \dots k_T\}$ starting from the origin link k_0 and terminating at link $k_T = d$.
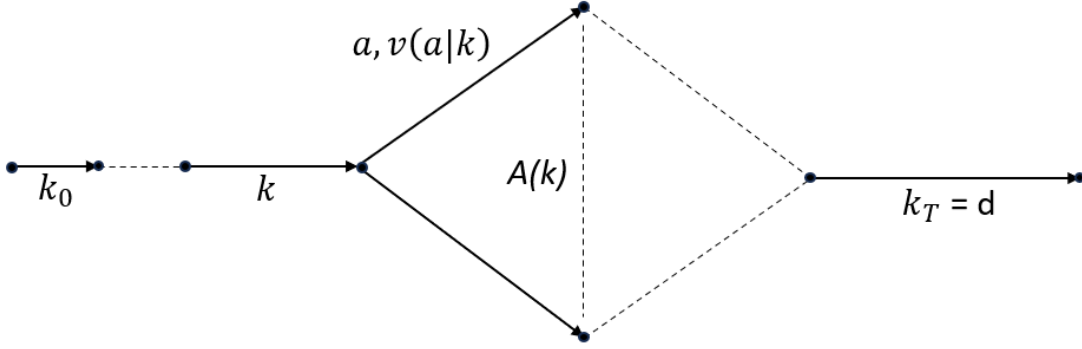
Figure 5. Illustration of Notation

From the MDP perspective, Rust (1994) first describes the inverse problem of recovering the utility function as a parameter estimation problem. The noise in the observed route data is captured by a random error term ε_a added to the systematic utility $v(a|k)$ resulting in: $v(a|k) + \mu\varepsilon_a$; μ is the scale parameter of the error term. The attributes in the model link-additive; the utility of a path is the summation of the link utilities of the path. Like the RUM framework, we assume the traveler chooses the route that maximizes their utility. From the perspective of the analyst, the traveler's behavior is consistent with solving a stochastic shortest path problem. Within this context, the *Bellman equation*, from the dynamic programing class of problems, gives the optimal *value function* when state is link *k* and realizations $e_{a\in\mathcal{A}(k)}$ of $\varepsilon_{a\in\mathcal{A}(k)}$ (Fosgerau et al., 2013; Zimmerman and Frejinger, 2020; Zimmermann et al., 2017):

$$V^d(k, e_a) = \begin{cases} 0 & , k = d \\ \max_{a\in\mathcal{A}(k)}[v(a|k) + \mu e_a + \int V^d(a, e_a)f(de_a)], & \forall k \in \mathcal{A} \end{cases} \qquad (Eq.\,1)$$

Eq. 1 can be simplified by taking the expectation with respect to ε_a and defining the expected value function as $V^d(k) = \int V^d(a, e_a)f(de_a)$ of state *k*, which gives:

$$V^d(k, e_a) = \begin{cases} 0 & , k = d \\ \max_{a\in\mathcal{A}(k)}[v(a|k) + \mu\varepsilon_a + V^d(a)], & \forall k \in \mathcal{A} \end{cases} \qquad (Eq.\,2)$$

To be consistent with other studies (Fosgerau et al. 2013; Zimmerman and Frejinger, 2020; Zimmermann et al. 2017) we refer to Eq. 2 as the *value function*. The analyst does not observe the utility function. From the analyst's perspective, the observe route choice behavior follows a probability distribution over a set of actions that maximize the expected utility (Eq. 2). Different assumptions on the error term ε_a lead to different functional forms for the transition probabilities $P^d(a|k)$. Given the assumption that ε_a is distributed *Extreme Type 1*, the probability takes on the familiar logit form and the recursive model is a recursive logit (RL):

$$P_n^d(a|k;\beta) = \frac{exp\left[\frac{1}{\mu}\left(v_n(a|k;\beta) + V_n^d(a|\beta)\right)\right]}{\sum_{a'\in A(k)} exp\left[\frac{1}{\mu}\left(v_n(a'|k;\beta) + V_n^d(a'|\beta)\right)\right]} \qquad (Eq.3)$$

where β is the parameter for link attributes. Given observed routes, the model can be estimated by maximum likelihood. When applying the recursive logit, the choice of path is formulated as a sequence of link choices (Fosgerau et al. 2013; Zimmermann et al. 2017) and the choice probabilities for a route $\sigma_n = \{k_0, k_1, k_2, \dots k_T\}$ are given by:

$$P(\sigma_n|\beta) = \prod_{j=1}^{T-1} P^d\left(k_{j+1}|k_j;\beta\right) \qquad (Eq.4)$$

As a result, the likelihood function for a set of N path observations is:

$$\mathcal{L}(\beta) = \prod_{n=1}^{N} P(\sigma_n|\beta) \qquad (Eq.5)$$

Link Size: In real-world networks, paths between a given origin and destination pair may share common links. This suggests that there exist unobserved correlations between path and the path utilities are correlated (Fosgerau et al. 2013). The *path size logit* formulation is a commonly used method to correct utility for overlapping paths. However, path size logit is not applicable in this recursive logit formulation; the recursive logit formulation requires link additive attributes, but the path size logit is not link additive. Fosgerau et al. (2013) proposed a link additive correction attribute called Link Size to correct utilities for overlapping links. The calculation of link size employs the anticipated link flow as an indicator of the degree of overlap. The anticipated link flow can be calculated by solving the following linear equation system:

$$(\boldsymbol{I} - \boldsymbol{P}^T)\boldsymbol{F} = \boldsymbol{G} \qquad (Eq.6)$$

where $\boldsymbol{I}$ is the identity matrix, $\boldsymbol{P}$ is the link choice probability matrix, $\boldsymbol{G}$ is the demand between an origin and destination pair, and $\boldsymbol{F}$ is the anticipated link flow.

CHAPTER 4. MODELING RESULTS

In this section, we present estimation results from the recursive logit route choice model. The recursive logit model estimation was completed using the MATLAB script from Mai (2016). The trust region method with an initial trust region radius equal to 1.0 and BGFS algorithm were used in the optimization of log-likelihood function (log of Eq. 4). The stopping condition for the program was reached by maximum number of iterations or the tolerance of gradient. The maximum number of iterations was set to 1,500 and the gradient tolerance was set to 1×10^{-6}. The estimation results based on this data are presented in Table 4.

The specification for Model 1 includes only distance, noise level, and link size, which accounts for path overlap. The coefficients for both distance and noise levels are negative, indicating that for a given OD pair, travelers on campus tend to choose routes with shorter distances and less noise, with a decibel of noise causing less disutility than a meter of distance. The specification for Model 2 includes all attributes. Link attributes that are qualitative, such as links traversing a tree canopy or that are paved sidewalk, were specified as a binary indicator (1/0) and interacted with both distance and noise level. The coefficient signs for both distance and noise remain negative with similar relative magnitudes, indicating similarity in tradeoffs from Model 1. Travel distance interacted with the parking lot binary indicator was statistically insignificant. Although we expect links that traverse a parking lot to statistically explain route choices, the estimation results from Model 2 indicate this is not the case. Similarly, noise interacted with the sidewalk and tree canopy were statistically insignificant at a 5% significance level. The interpretation is that each decibel of noise experienced on links traversing sidewalks and tree canopies do not statistically differ from each other.

Table 4: Route Choice Model Estimation Results

Coefficient	Model 1			Model 2			Model 3		
	Value	Std. Error	t-statistic	Value	Std. Error	t-statistic	Value	Std. Error	t-statistic
Travel Distance (100 meters)	-4.852	0.389	-12.468	-6.040	0.674	-8.960	-5.768	0.562	-10.259
Noise (10 db)	-0.054	0.007	-8.058	-0.044	0.023	-1.888	-0.059	0.009	-6.710
Link Size	-0.411	0.054	-7.605	-0.406	0.065	-6.254	-0.408	0.064	-6.369
Interaction Terms									
Travel Distance - Sidewalk (1/0)	---	---	---	1.157	0.440	2.630	0.903	0.258	3.493
Travel Distance - Non-Paved (1/0)	---	---	---	3.639	1.338	2.719	3.392	1.280	2.650
Travel-Distance - Plaza/Quad (1/0)	---	---	---	-0.794	0.311	-2.555	-0.779	0.312	-2.498
Travel Distance - Tree Canopy (1/0)	---	---	---	0.461	0.223	2.063	0.298	0.129	2.312
Travel Distance - Parking Lot (1/0)	---	---	---	1.471	1.759	0.836	---	---	---
Noise- Sidewalk (1/0)	---	---	---	-0.014	0.022	-0.643	---	---	---
Noise - Grass (1/0)	---	---	---	-0.153	0.090	-1.711	-0.138	0.085	-1.620
Noise - Quadrangle (1/0)	---	---	---	0.036	0.011	3.318	0.035	0.011	3.241
Noise - Tree Canopy (1/0)	---	---	---	-0.010	0.011	-0.941	---	---	---
Noise - Parking Lot (1/0)	---	---	---	0.135	0.087	1.560	0.207	0.028	7.326
Sample Size (Travelers)	16			16			16		
Sample Size (Routes)	298			298			298		
Sample Size (Links)	5,404			5,404			5,404		
LL(0)	-4280.479			-4280.479			-4280.479		
LL(β)	5.704			5.622			5.621		
Run Time (min)	15			150			70		

The specification for Model 3 only includes variables from Model 2 that were statistically significant. First, all the coefficients of variables retained were still statistically significant, retained their signs, and had similar magnitudes. Distance and noise continue to have negative coefficients, indicating a disutility for both, as each one increases in quantity. The positive signs for distance interacted with sidewalk, grass, and tree canopy indicate that, per distance, these infrastructure surfaces will improve a traveler's utility relative to other attributes, but at different levels. Overall, grass leads to a higher utility per distance, relative to other attributes, followed by sidewalk and tree-canopy. Travelers prefer shorter and quitter routes, given a specific OD pair. Links that traverse grass tend to be more direct and shorter in distance on campus, compared to a sidewalk counterpart, which tend to be more rectilinear and less direct. Interestingly, the interaction term between distance and quadrangle is negative, indicating these links were avoided, relative to other link attributes. One possible explanation could be the noisy nature of quadrangles, as a gathering location for students.

The negative signs for the interaction term between noise and grass surfaces indicate that while noise is negatively perceived, noise experienced while walking on grassy surfaces lead to even greater disutility. This is consistent with Travelers preferring shorter and quieter routes, given a specific OD pair. Interestingly, the interaction term between noise and quadrangle crossings has a positive sign, giving a net utility of -0.024 (-0.059 + 0.035), indicating the per decibel disutility from noise is reduced. This indicates an improvement in utility over other attributes. One explanation could be that noise is expected in a quadrangle setting. The interaction term between noise and parking lot also has a positive sign and large magnitude, giving a positive net utility of 0.15, which suggests that noise has a positive impact in parking lot areas. Similar to the interaction variable of noise with traversing a quadrangle, the positive impact could be because parking lots are inherently noisier environments, and the noise expectation might be more tolerable.

Figure 7 shows the *marginal disutility* per unit of distance for all the attributes from Model 3. The presence of sidewalk, grass surface, tree canopy coverage can compensate for the disutility created by distance on its own. Thus, while pedestrians experience a disutility for longer routes, this can be offset by making the surface paved as a sidewalk, providing a grassy surface or more shade from tree canopy coverage. Only the quadrangle attribute resulted in a *greater net disutility* with respect to distance; this is possibly because traversing a quadrangle leads to longer sun exposure and more crowds. Based on the marginal disutility in Figure 7, the design of walking paths benefits from grass surfaces, followed by sidewalks and tree canopy, in terms of infrastructure. While investments in all three types would offset the base disutility from distance, having grassy surfaces appears to yield the most benefit in terms of increasing the likelihood of a walking path being used.
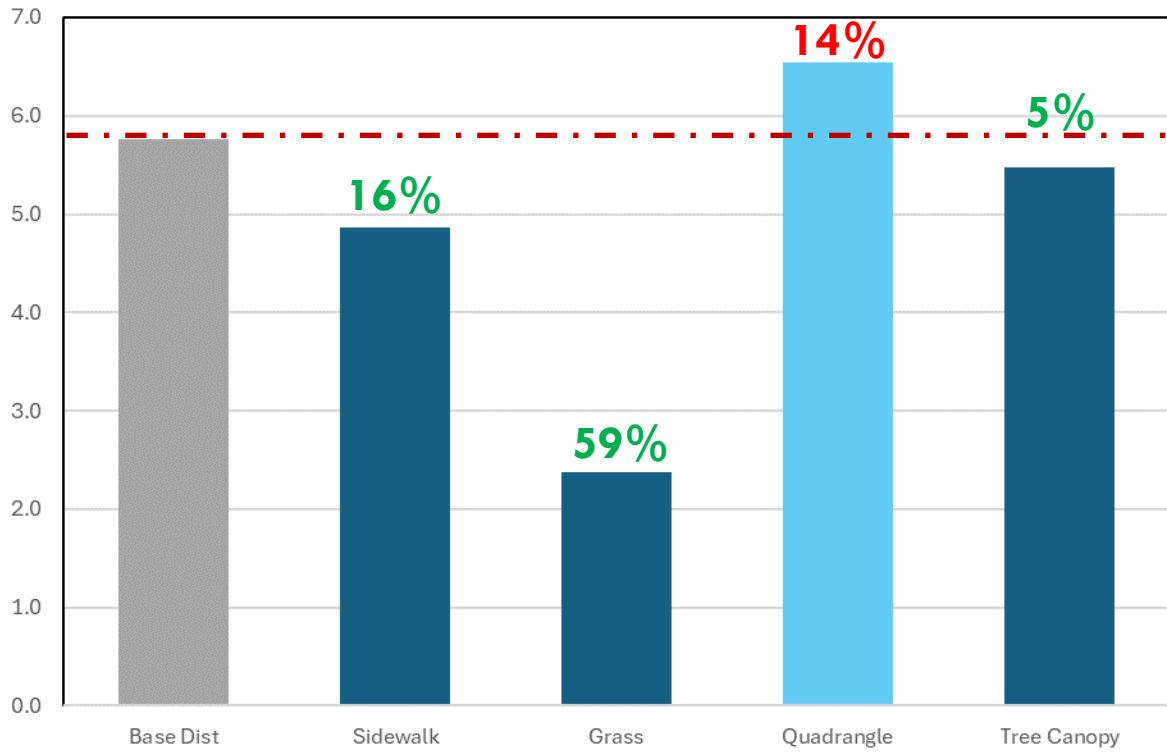
Figure 6. Marginal Disutility (per 100 meters)

CHAPTER 5. APPLICATION AT SKYLINE STATIONS

In this section, we present the constructed pedestrian network at each identified Skyline station and the application of calibrated recursive logit model to analyze pedestrian flow distribution on the pedestrian network. The developed pedestrian network construction framework and discrete choice model were applied to the four selected Skyline Stations, Waiawa Pearl Highlands Station, Pouhala Waipahu Transit Center Station, Kualaka'i East Kapolei Station, and Keone'ae U.H. West Oahu Station, as shown in Figure 7.
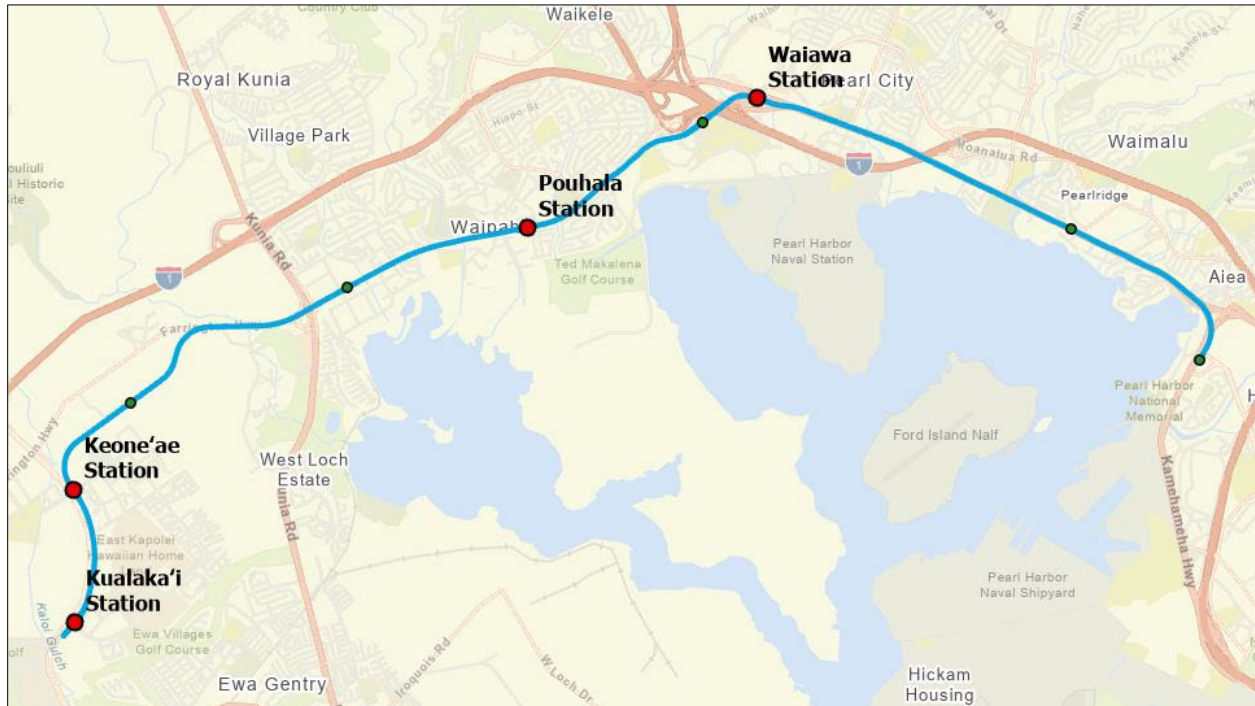
Figure 7. Location of Selected Skyline Station in Honolulu

The network contains links and nodes. Each link represents a walkable way, this can be sidewalks, crosswalks, pedestrian pathways, pedestrian cross bridges, etc. Each node represents an end point of a link, this could be intersection of links or a terminal node of a link. For major streets, such as arterial roads and collector roads, specific links were constructed for sidewalks on both sides of the street to explicitly account for the pedestrian traffic on both sides of the street. For areas like university campuses, the pedestrian network also includes pedestrian pathways through yards and quadrangles.

An individual pedestrian network was developed for each station. The pedestrian network was designed to cover areas around the station within walking distance. The network will cover the common destinations near the Skyline station, such as shopping centers, residential communities, education facilities, post office, recreational facilities, etc. The network was initially acquired from OpenStreetMap. Then, the network was updated by using Google satellite image to include all currently available pedestrian facilities, such as sidewalks, crosswalks, and cross bridges. The pedestrian networks for each of the four stations are demonstrated in Figure 7, Figure 8, Figure 9, and Figure 10. The network attributes for identified Skyline station are summarized in Table 5.

Table 5: Network Characteristics at Skyline Stations

Waiawa Pearl Highlands Station

Network Attributes		Percentage of Network Distance by Attribute	
Number of Links	124	Paved Sidewalk	81.0%
Number of Nodes	100	Grassy Surface	0.4%
Total Distance (meters)	10,121	Quadrangle	0%
		Tree Canopy	4.2%
		Parking Lot	3.7%

Pouhala Waipahu Transit Center Station

Network Attributes		Percentage of Network Distance by Attribute	
Number of Links	253	Paved Sidewalk	49.4%
Number of Nodes	210	Grassy Surface	0%
Total Distance (meters)	13,900	Quadrangle	0%
		Tree Canopy	0%
		Parking Lot	16.4%

Kualaka'i East Kapolei Station

Network Attributes		Percentage of Network Distance by Attribute	
Number of Links	152	Paved Sidewalk	90.6%
Number of Nodes	117	Grassy Surface	0%
Total Distance (meters)	8,357	Quadrangle	9.1%
		Tree Canopy	0%
		Parking Lot	1.0%

Keone'ae U.H. West Oahu Station

Network Attributes		Percentage of Network Distance by Attribute	
Number of Links	215	Paved Sidewalk	83.0%
Number of Nodes	156	Grassy Surface	0%
Total Distance (meters)	12,703	Quadrangle	9.2%
		Tree Canopy	3.4%
		Parking Lot	2.9%
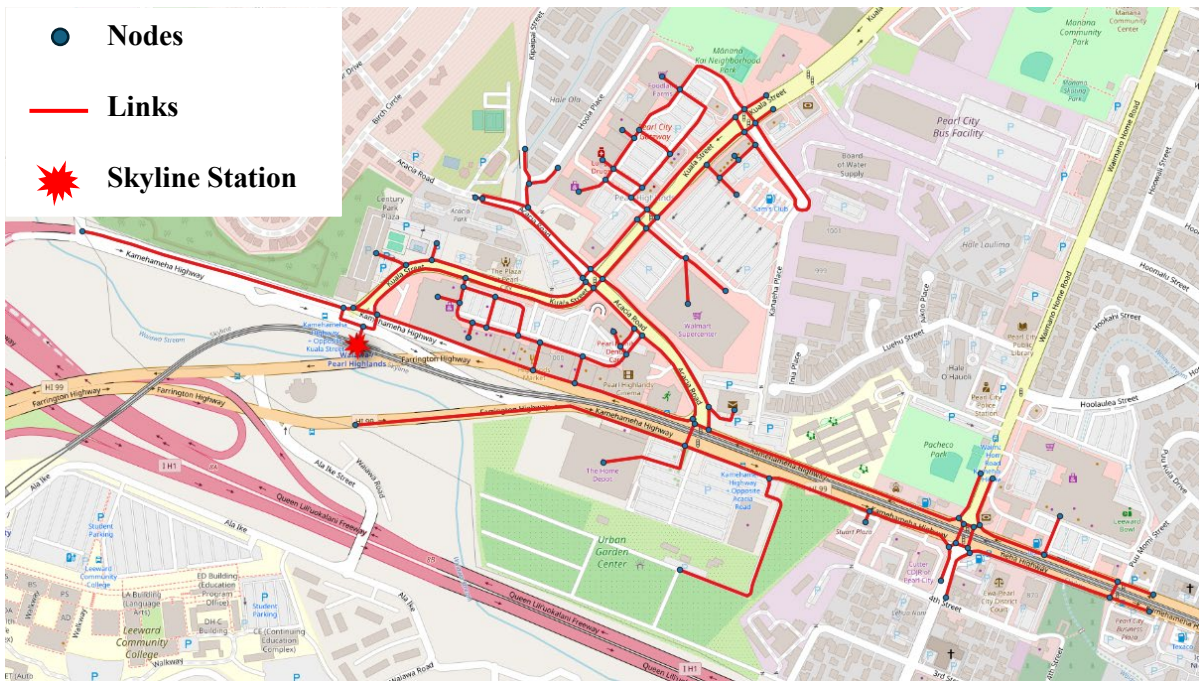
Figure 8. Pedestrian Network for Waiawa Pearl Highlands Station
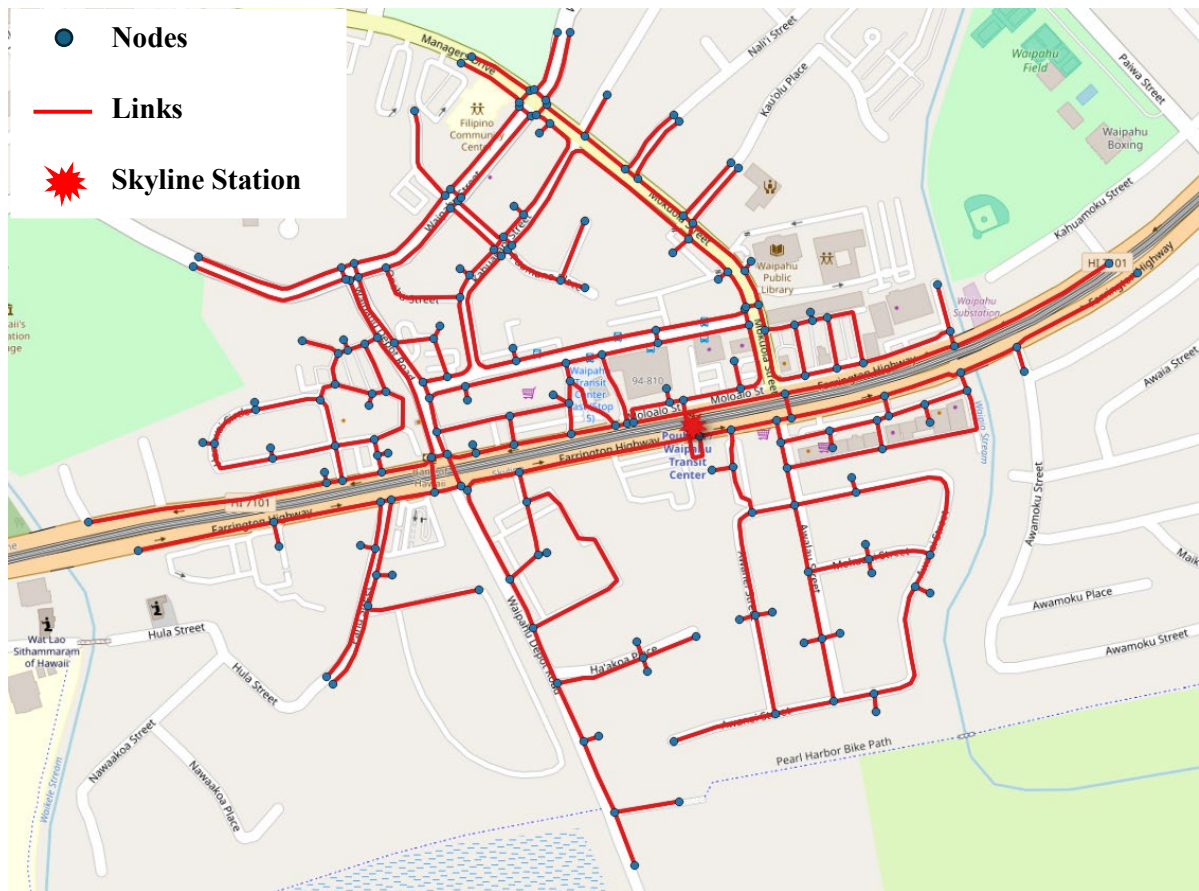
Figure 9. Pedestrian Network for Pouhala Waipahu Transit Center Station

Figure 10. Pedestrian Network for Kualaka'i East Kapolei Station

Figure 11. Pedestrian Network for Keone'ae U.H. West Oahu Station

10 OD pairs were selected for each station for pedestrian flow distribution analysis. The main goal is to analyze the pedestrian flow leaving or entering the station. The destination for all OD pairs will always be the Skyline station. Popular points of interests on the network were selected as the origins, such as supermarkets, shopping centers, business plazas, residential communities, educational facilities, etc. Detailed information for each selected OD pairs is presented in Table 6.

Table 6: Description of Selected OD Pairs

Waiawa Pearl Highlands Station

Origin	Destination
Walmart on Kuala St	Waiawa Pearl Highlands Station
Century Park Plaza	Waiawa Pearl Highlands Station
Acacia Rd. and Kipaipai St	Waiawa Pearl Highlands Station
Longs Drugs on Kuala St	Waiawa Pearl Highlands Station
Restaurants Near Sam's Club Gas Station	Waiawa Pearl Highlands Station
USPS Office on Kamehameha Hwy	Waiawa Pearl Highlands Station
The Home Depot on Kamehameha Hwy	Waiawa Pearl Highlands Station
Pearl City Shopping Center	Waiawa Pearl Highlands Station
Sam's Club	Waiawa Pearl Highlands Station
Stuart Plaza	Waiawa Pearl Highlands Station

Pouhala Waipahu Transit Center Station

Origin	Destination
Times Supermarket – Waipahu	Pouhala Waipahu Transit Center Station
Waipahu St and Waipahu Depot St	Pouhala Waipahu Transit Center Station
Waipahu Public Library	Pouhala Waipahu Transit Center Station
Farrington Hwy + Opp Mokuola St Shops	Pouhala Waipahu Transit Center Station
Waipahu St and Mokuola St	Pouhala Waipahu Transit Center Station
Waipahu United Church of Christ	Pouhala Waipahu Transit Center Station

Pahu St.	Pouhala Waipahu Transit Center Station
Waipahu Festival Marketplace	Pouhala Waipahu Transit Center Station
Puamano Place and Kahiki Place	Pouhala Waipahu Transit Center Station
Awalau St and Mokuahi St	Pouhala Waipahu Transit Center Station

Kualaka'i East Kapolei Station

Origin	Destination
The Salvation Army Kroc Center Hawaii	Kualaka'i East Kapolei Station
Kaneoneo St	Kualaka'i East Kapolei Station
Residentials on South Keahumoa Pkwy	Kualaka'i East Kapolei Station
Kapolei Elementary School	Kualaka'i East Kapolei Station
'Elepu'u St and Kumuhonua St	Kualaka'i East Kapolei Station
Building F Honouliuli Middle School	Kualaka'i East Kapolei Station
Football Field Honouliuli Middle School	Kualaka'i East Kapolei Station
Kualakai Pkwy station north	Kualaka'I East Kapolei Station
Keahumoa Pkwy and Maweke St	Kualaka'i East Kapolei Station
Maunakapu St and Maweke St	Kualaka'i East Kapolei Station

Keone'ae U.H. West Oahu Station

Origin	Destination
U.H. West Oahu Administration Building	Keone'AE U.H. West Oahu Station
U.H. West Oahu Library	Keone'AE U.H. West Oahu Station
Hawaii Tokai International College	Keone'AE U.H. West Oahu Station
U.H. West Oahu Recreation Center	Keone'AE U.H. West Oahu Station
Nana Hope St Residentials	Keone'AE U.H. West Oahu Station
Nana Hope St and 'Ōnohiʻula St Residentials	Keone'AE U.H. West Oahu Station
Ho'omohala Ave and Kauluakoko St	Keone'AE U.H. West Oahu Station

Kauluakoko St and 'Ōnohi'ula St	Keone'AE U.H. West Oahu Station
Ho'okulāia St and Kauluakoko St	Keone'AE U.H. West Oahu Station
Kulanihakoi St and Kauluakoko St	Keone'AE U.H. West Oahu Station

To analyze the flow distribution across the network for selected OD pairs, a pedestrian travel demand needs to be assigned to each OD pair. Filed surveys focusing on pedestrian traffic were conducted at selected Skyline stations. However, the Skyline Rail is still at its early operation stage, the current ridership might not be sufficient to reflect the actual pedestrian trips from and to the station. The results from the field surveys are not sufficient to determine the pedestrian travel demands associated with Skyline stations. Hence, we assumed 100 pedestrian trips per day for each OD pair.

At each selected Skyline station, the calibrated recursive logit model was applied to determine the flow distribution for each specific OD pair. We used the coefficients from Model 3, which is model with only statistically significant coefficients. For each OD pair, the RL model will calculate and distribute flows to each link in the network. The flow distribution was calculated for each of the 10 OD pairs, then the flow on each link was added at link level to calculate the total flow on each link. This process was repeated at all selected stations. At the end of this stage, the total pedestrian flow distribution at each link for all 4 networks was determined. Visualizations for total pedestrian flow distribution on the constructed network at each station are demonstrated in Figure 11 (a), Figure 12 (a), Figure 13 (a), and Figure 14 (a). Figure 11 (b), Figure 12 (b), Figure 13 (b), and Figure 14 (b) present a zoom in visualization just focusing on the areas next to the stations, the numbers shown in these figures are the pedestrian flow numbers on each link.
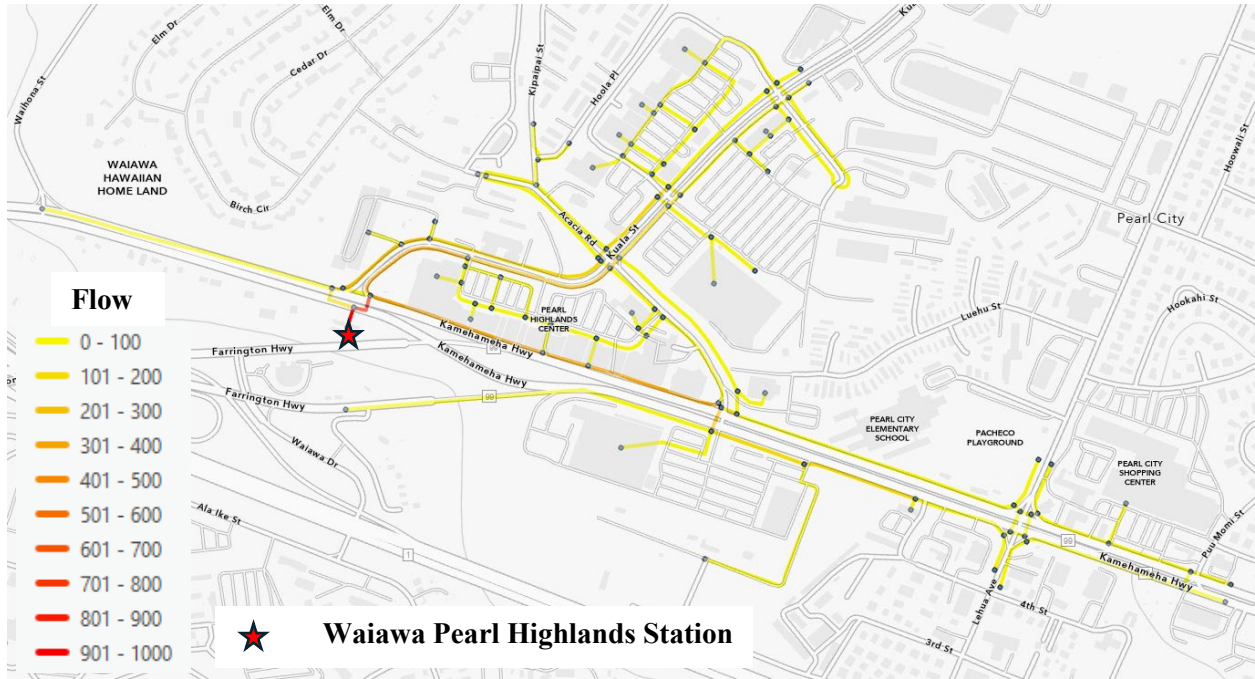
Figure 12 (a). Pedestrian Flow Distribution at Waiawa Pearl Highlands Station
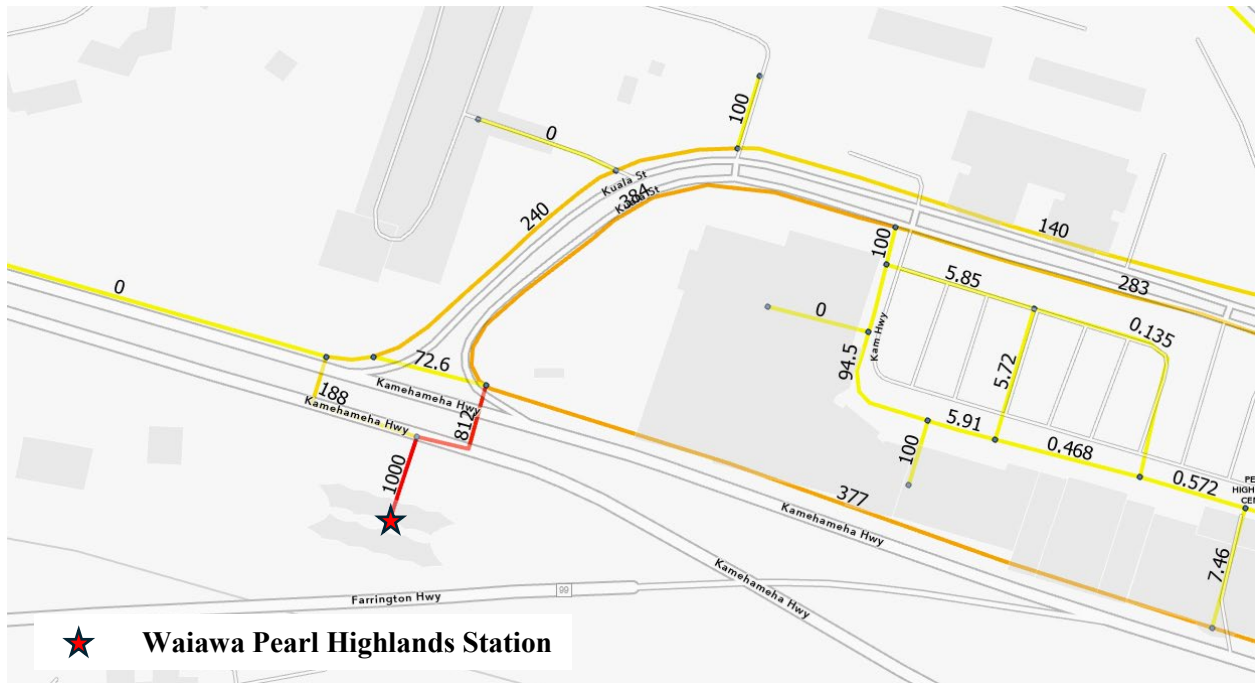
Figure 12 (b). Pedestrian Flow Distribution at Waiawa Pearl Highlands Station (Zoom in to Station Area)
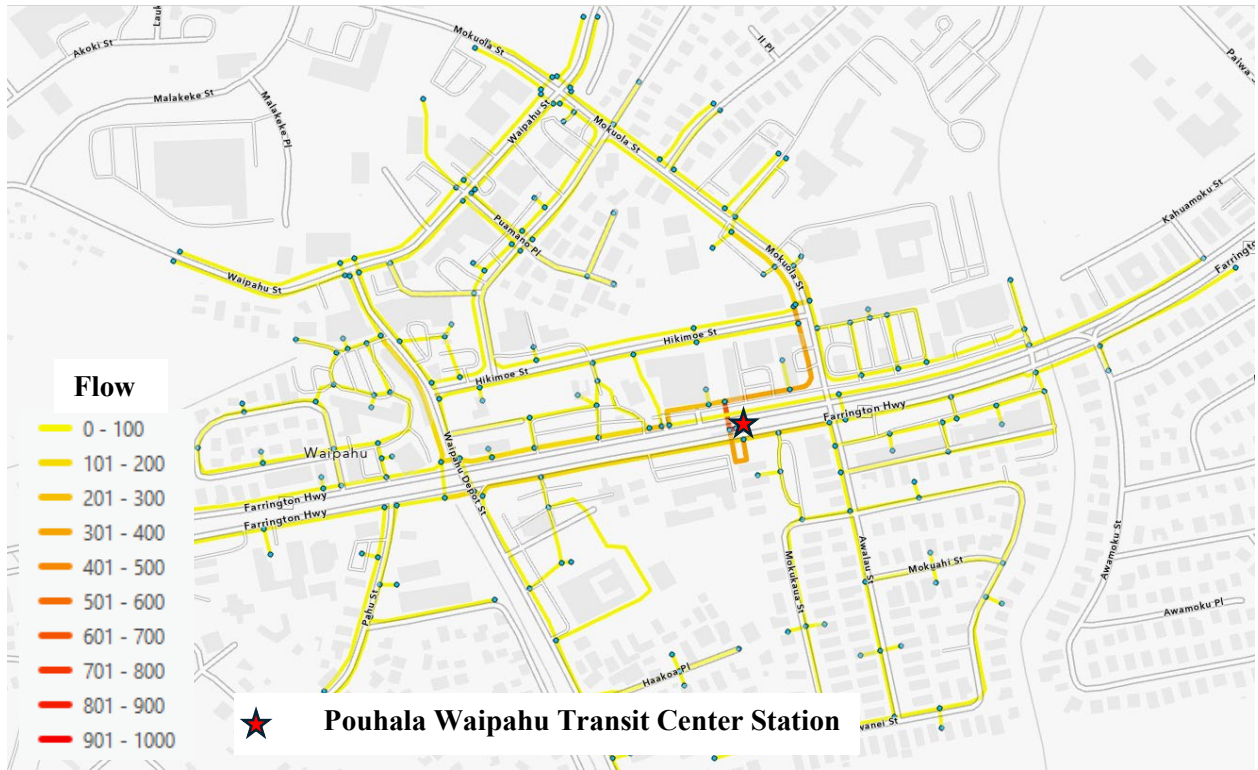
Figure 13 (a). Pedestrian Flow Distribution at Pouhala Waipahu Transit Center Station
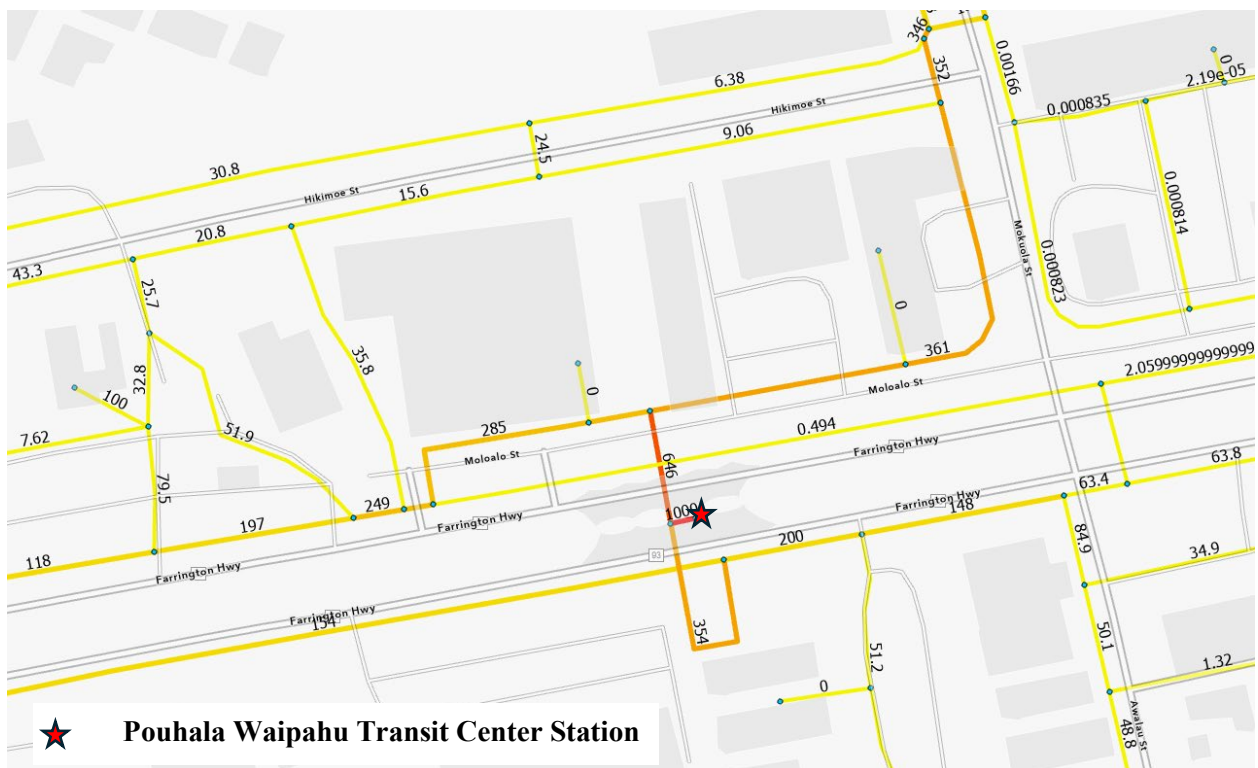
Figure 13 (b). Pedestrian Flow Distribution at Pouhala Waipahu Transit Center Station (Zoom in to Station Area)
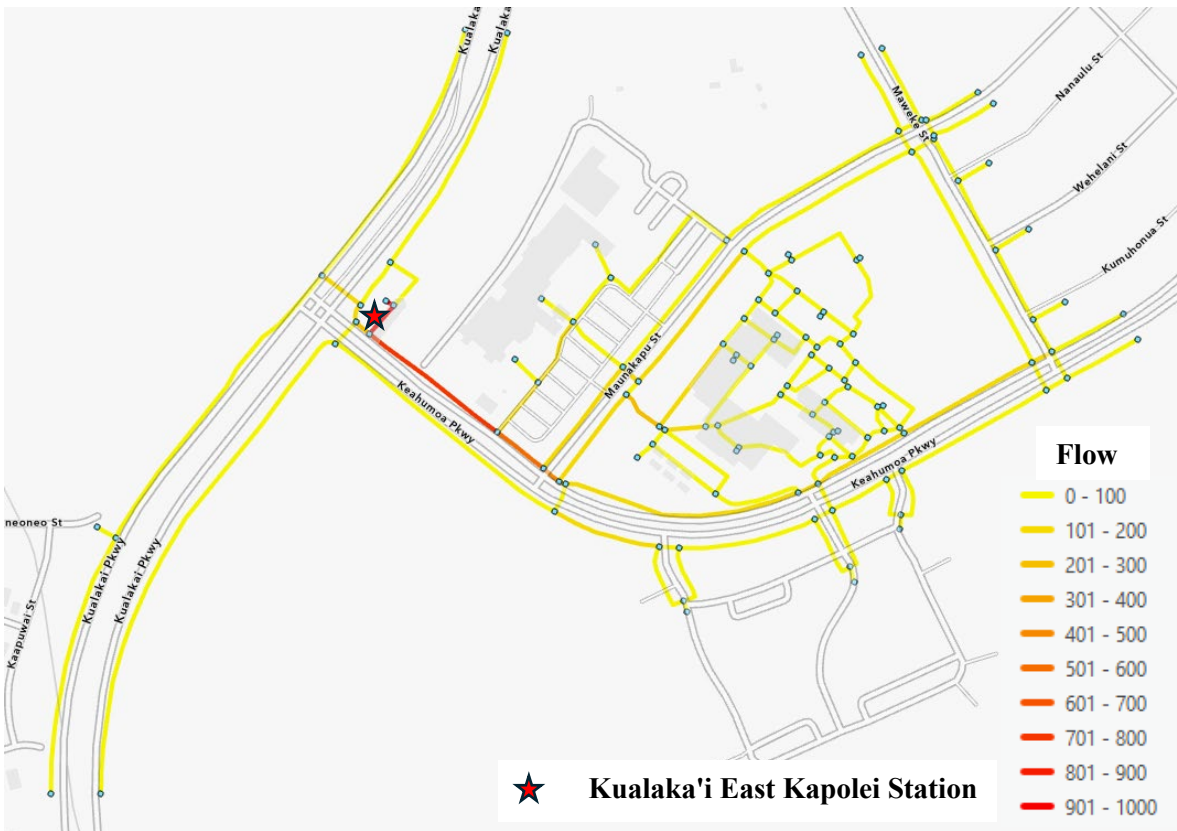
Figure 14 (a). Pedestrian Flow Distribution at Kualaka'i East Kapolei Station

Figure 14 (b). Pedestrian Flow Distribution at Pouhala Waipahu Transit Center Station (Zoom in to Station Area)
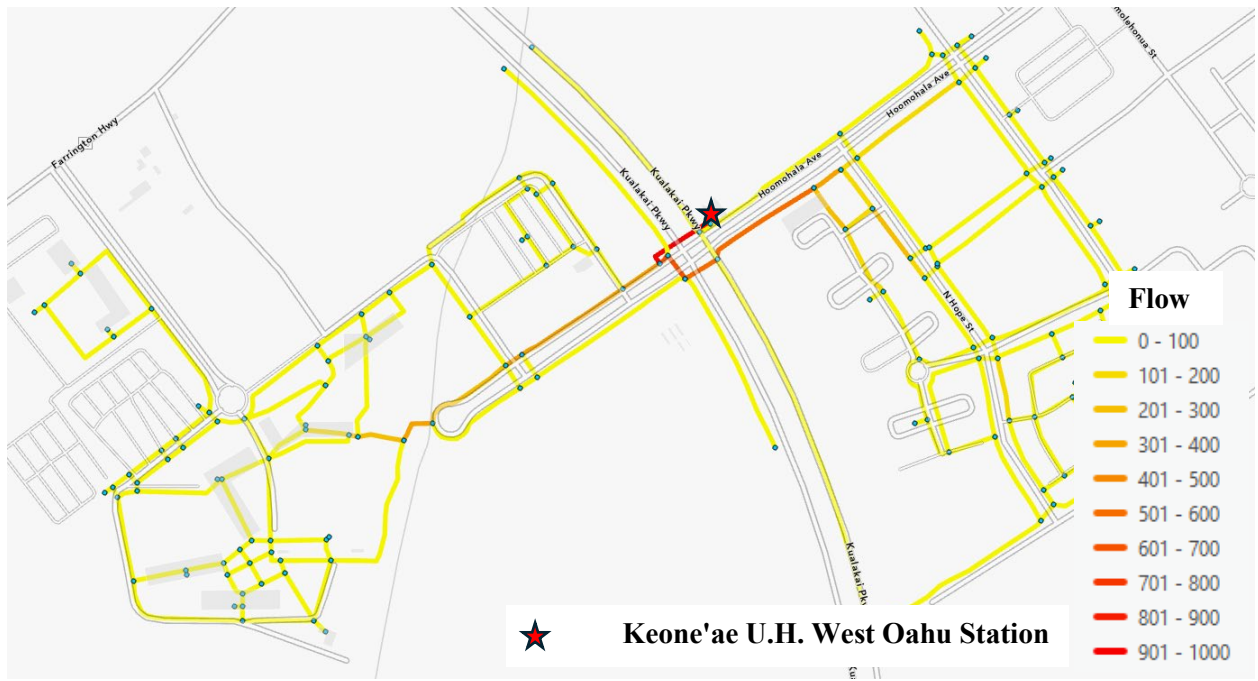
Figure 15 (a). Pedestrian Flow Distribution at Keone'ae U.H. West Oahu Station
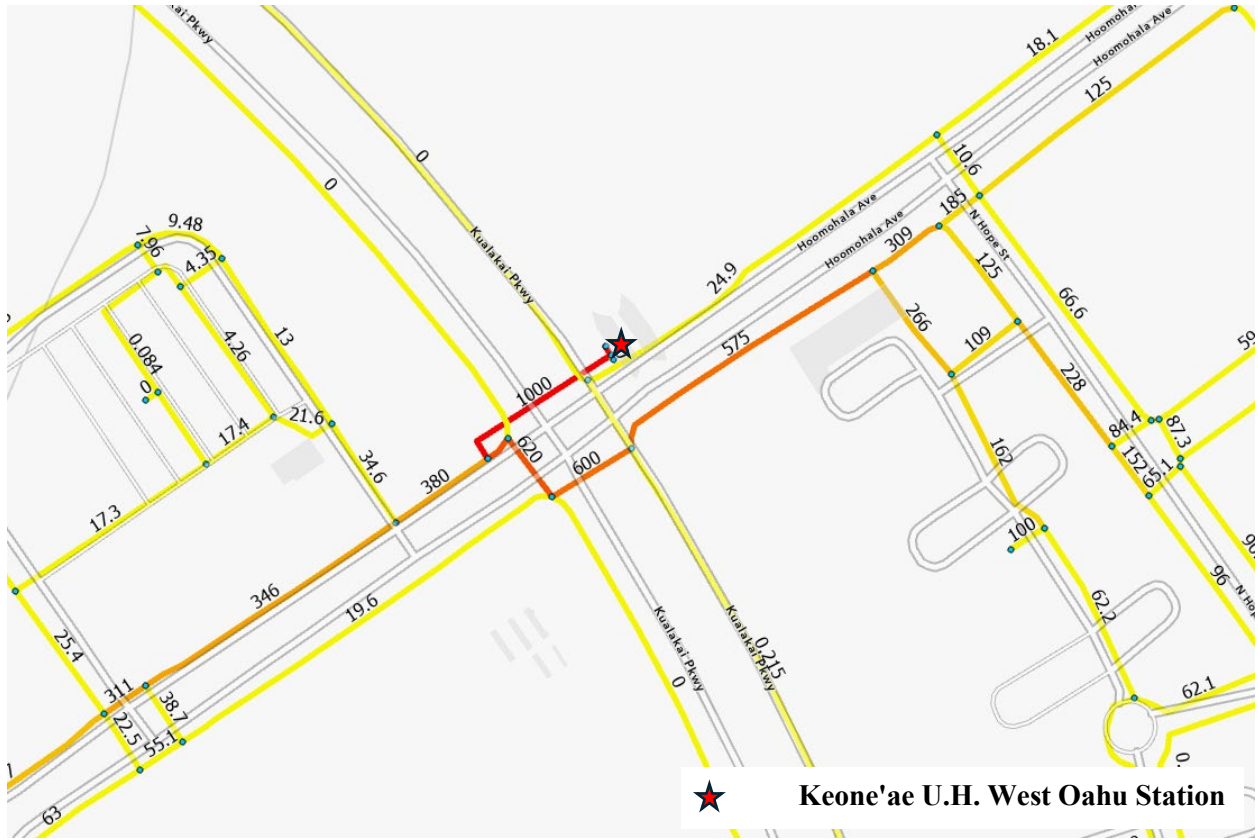
Figure 15 (b). Pedestrian Flow Distribution at Keone'ae U.H. West Oahu Station (Zoom in to Station Area)

At Waiawa Pearl Highlands Station, most of the pedestrian traffic will come from the north side of the Kamehameha Highway, where the residential buildings and shopping centers are located. Pedestrians coming from the north of the Kamehameha Highway need to cross the Kamehameha Highway to access the Waiawa Pearl Highway Station. Pedestrians coming from the shops or communities on the south side of Kamehameha Highway, such as The Home Depot, will most likely cross the Kamehameha Highway first and walk along the sidewalk on west bound side of the Kamehameha Highway. This is because the Farrington Highway intersects Kamehameha Highway from the south, the intersection leaves the east bound side of Kamehameha Highway with no continuous sidewalk. Hence, most of the pedestrian traffic accessing the Skyline station need to cross Kamehameha Highway and the intersection of Kamehameha Highway and Kuala Street. Based on the simulation results, about 80% of the pedestrian traffic will cross on the east side of the Kamehameha Highway and Kuala Street intersection.

The Pouhala Waipahu Transit Center Station is surrounded by residential communities, commercial facilities, and shopping plazas. All these locations might generate pedestrian trips to the Skyline station. Pedestrian crossing bridges have been constructed at both sides of the Farrington Highway. All pedestrian traffic accessing the station will need to use the pedestrian crossing bridge from either side of the Farrington Highway. For pedestrians accessing the station from the east, if they are walking on the north side of the Farrington Highway, they may walk on the sidewalk on Moloalo Steet, and cross Mokuola Street. However, the intersection of Moloalo Street and Mokuola Street does not have a crosswalk marking, which might induce safety concerns.

The Kualaka'i East Kapolei Station is in a rural and suburban area. Pedestrian traffic accessing this station might come from the residential community on the southeast, and communities and education facilities along the Keahumoa Pkwy. The station is only accessible at the intersection of Kualakai Pkwy and Keahumoa Pkwy. Pedestrian traffic from the community on the southeast side of the station will walk along Kualakai Pkwy and cross the Kualakai Pkwy in front of the station. Pedestrian traffic coming from Honouliuli Middle School and nearby communities will merge at Keahumoa Pkwy before arriving at the station.

The Keone'ae U.H. West Oahu Station is at the intersection of Kualakai Pkwy and Ho'omohala Ave. At this Station, pedestrian traffic will come from the UH West Oahu on the west, and the residential communities on the east. A park and ride option is available at this station, pedestrian traffic is expected from the park and ride parking lot. Pedestrian traffic from the UH West Oahu campus will access the station via Ho'omohala Ave. A pedestrian crossing bridge is constructed from the northwest corner of the intersection to the station. All pedestrians will need to use this crossing bridge to access the station. It appears that there is no station entrance on the east side of the Kualakai Pkwy. On the other hand, at the intersection, crosswalk is only available on the south side of Ho'omohala Ave, while the station is on the north side of Ho'omohala Ave. This means pedestrian traffic from Ho'omohala Ave will need to cross the Kualakai Pkwy and Ho'omohala Ave at grade level to access the station. Kualakai Pkwy is a multilane busy highway, which may cause safety risks for pedestrians even with crosswalks.

CHAPTER 6. CONCLUSIONS

To analyze the pedestrian flow distribution near the identified Skyline stations. We first conducted a study on pedestrian route choice behavior at the University of Hawaii at Manoa campus. In this study, we estimate a recursive logit model based on observed route choices from volunteers on a university campus who logged GPS points for two weeks. The recursive logit model is a link-based model, which formulates the route choice problem as link choice problem at each node. The estimation results indicate that sidewalks, grass surfaces, and a tree canopy are preferred over links that traverse quadrangles. Pedestrians have a higher likelihood of choosing a route with more sidewalks, grass surface and less sun exposure. With respect to noise, traversing quadrangles and parking lots is preferable than sidewalks, grass surface, and tree canopy.

An individual pedestrian network was constructed for each identified Skyline station to cover the point of interests in walking distance. Ten OD pairs were selected for pedestrian flow distribution analysis at each station. We applied our final model specification (Model 3) to calculate the pedestrian flow distribution on the network. Pedestrian traffic needs to cross major highways to access the station at Waiawa Pearl Highlands Station, Kualaka'i East Kapolei Station, and Keone'ae U.H. West Oahu Station. As the Skyline ridership increases in the future, this might become a higher risk to pedestrian safety.

REFERENCES

Aumond, P., Can, A., Mallet, V., De Coensel, B., Ribeiro, C., Botteldooren, D., and Lavandier, C. (2018). Kriging-based spatial interpolation from measurements for sound level mapping in urban areas. The Journal of the Acoustical Society of America, vol. 143(5), pp. 2847-2857.

Azevedo, J., Costa, M. E. O. S., Madeira, J. J. E. S., & Martins, E. Q. V. (1993). An algorithm for the ranking of shortest paths. European Journal of Operational Research, vol. 69(1), pp. 97-106.

Barra, T.D., Pérez, B., & Anez, J. (1993). Multidimensional path search and assignment. Presented at 21st PTRC Summer Annual Meeting, Manchester, United Kingdom, 1993.

Basu, N., Haque, M. M., King, M., Kamruzzaman, M., & Oviedo-Trespalacios, O. (2022). A systematic review of the factors associated with pedestrian route choice. Transport Reviews, 4 vol. 2(5), pp. 672-694.

Basu, R., & Sevtsuk, A. (2022). How do street attributes affect willingness-to-walk? City-wide pedestrian route choice analysis using big data from Boston and San Francisco. Transportation Research Part A: Policy and Practice, vol. 163, pp. 1-19.

Bekhor, S., Ben-Akiva, M. E., & Ramming, M. S. (2006). Evaluation of choice set generation algorithms for route choice models. Annals of Operations Research, vol. 144, pp. 235-247.

Ben-Akiva, M., Bergman, M. J., Daly, A. J., & Ramaswamy, R. (1984). Modelling inter urban route choice behaviour. In Papers presented during the Ninth International Symposium on Transportation and Traffic Theory held in Delft the Netherlands, 11-13 July 1984.

Bovy, P. H., & Stern, E. (2012). Route choice: Wayfinding in transport networks: Wayfinding in transport networks (Vol. 9). Springer Science & Business Media.

Broach, J., Dill, J., & Gliebe, J. (2012). Where do cyclists ride? A route choice model developed with revealed preference GPS data. Transportation Research Part A: Policy and Practice, vol. 46(10), pp. 1730-1740.

Byon, Y. J., Abdulhai, B., & Shalaby, A. (2009). Real-time transportation mode detection via tracking global positioning system mobile devices. Journal of Intelligent Transportation Systems, vol. 13(4), pp. 161-170.

Casello, J. M., & Usyukov, V. (2014). Modeling cyclists' route choice based on GPS data. Transportation Research Record, vol. 2430(1), pp. 155-161.

Chen, J., Yang, S. T., Li, H. W., Zhang, B., & Lv, J. R. (2013). Research on geographical environment unit division based on the method of natural breaks (Jenks). The International Archives of the Photogrammetry, Remote Sensing and Spatial Information Sciences, vol. 40, pp. 47-50.

Ciscal-Terry, W., Dell'Amico, M., Hadjidimitriou, N. S., & Iori, M. (2016). An analysis of drivers route choice behaviour using GPS data and optimal alternatives. Journal of transport geography, vol. 51, pp. 119-129.

Clifton, K. J., Singleton, P. A., Muhs, C. D., & Schneider, R. J. (2016). Development of destination choice models for pedestrian travel. Transportation Research Part A: Policy and Practice, vol. 94, pp. 255-265.

Daamen, W., Bovy, P. H. L., & Hoogendoorn, S. P. (2002). Modelling pedestrians in transfer stations. Pedestrian and evacuation dynamics, pp. 59-73.

de Jong, T., & Fyhri, A. (2023). Spatial characteristics of unpleasant cycling experiences. Journal of transport geography, vol. 112, 103646.

Delso, J., Martín, B., Ortega, E., & Otero, I. (2017). A model for assessing pedestrian corridors. Application to Vitoria-Gasteiz City (Spain). Sustainability, vol. 9(3).

Department of Transportation Service, City and County of Honolulu. (2022). Oahu Pedestrian Plan. Honolulu, Hawaii.

EarthDefine LLC, US Forest Service, National Oceanic and Atmospheric Administration, Hawaii Division of Forestry and Wildlife. (2021). Hawaii High Resolution 1m Tree Canopy Map [ESRI file geodatabase raster format], 2009-2020. https://www.fs.usda.gov/detailfull/r5/communityforests/?cid=fseprd995876

Eppstein, D. (1998). Finding the k shortest paths. SIAM Journal on computing, vol. 28(2), pp. 652-673.

Feliciani, C., & Nishinari, K. (2018). Measurement of congestion and intrinsic risk in pedestrian crowds. Transportation Research Part C: Emerging Technologies, vol. 91, pp. 124-155.

Fleming, J., Honour, H., & Pevsner, N. (1980). The Penguin dictionary of architecture (3rd ed.). Penguin.

Fosgerau, M., Frejinger, E., & Karlstrom, A. (2013). A link-based network route choice model with unrestricted choice set. Transportation Research Part B: Methodological, vol. 56, pp. 70-80.

Ghanayim, M., & Bekhor, S. (2018). Modelling bicycle route choice using data from a GPS-assisted household survey. European Journal of Transport and Infrastructure Research, vol. 18(2).

Gundogdu, K. S., & Guney, I. (2007). Spatial analyses of groundwater levels using universal kriging. Journal of earth system science, vol. 116, pp. 49-55.

Guo, Z., & Loo, B. P. (2013). Pedestrian environment and route choice: evidence from New York City and Hong Kong. Journal of Transport Geography, vol. 28, pp. 124-136.

Guo, Z. (2009). Does the pedestrian environment affect the utility of walking? A case of path choice in downtown Boston. Transportation Research Part D: Transport and Environment, vol. 14(5), pp. 343-352.

Hawaii Department of Transportation. (2013). Statewide Pedestrian Master Plan. Honolulu, Hawaii.

Hoogendoorn, S. P., van Wageningen-Kessels, F., Daamen, W., Duives, D. C., & Sarvi, M. (2015). Continuum theory for pedestrian traffic flow: Local route choice modelling and its implications. Transportation Research Procedia, vol. 7, pp. 381-397.

Hoogendoorn, S. P., & Bovy, P. H. (2005). Pedestrian travel behavior modeling. Networks and Spatial Economics, vol. 5, pp. 193-216.

Hoogendoorn, S. P., & Bovy, P. H. (2004). Pedestrian route-choice and activity scheduling theory and models. Transportation Research Part B: Methodological, vol. 38(2), pp. 169-190.

Hu, J., Razdan, A., Femiani, J. C., Cui, M., & Wonka, P. (2007). Road network extraction and intersection detection from aerial images by tracking road footprints. IEEE Transactions on Geoscience and Remote Sensing, vol. 45(12), pp. 4144-4157.

Kasemsuppakorn, P., & Karimi, H. A. (2013). A pedestrian network construction algorithm based on multiple GPS traces. Transportation Research Part C: Emerging Technologies, vol. 26, pp. 285-300.

Lai, X., Fu, H., Li, J., & Sha, Z. (2019). Understanding drivers' route choice behaviours in the urban network with machine learning models. IET Intelligent Transport Systems, vol. 13(3), pp. 427-434.

Langley, R. B. (1999). Dilution of precision. GPS world, vol. 10(5), pp. 52-59.

Lue, G., & Miller, E. J. (2019). Estimating a Toronto pedestrian route choice model using smartphone GPS data. Traveler Behaviour and Society, vol. 14, pp. 34-42.

Lu, J., & Zhou, X. S. (2023). Virtual track networks: A hierarchical modeling framework and open-source tools for simplified and efficient connected and automated mobility (CAM) system design based on general modeling network specification (GMNS). Transportation Research Part C: Emerging Technologies, vol. 153, 104223.

Mai, T. (2016). RecursiveLogit.Classical.V2. https://github.com/maitien86/RecursiveLogit.Classical.V2

Merry, K., & Bettinger, P. (2019). Smartphone GPS accuracy study in an urban environment. PloS one, vol. 14(7).

Oliver, M. A., & Webster, R. (1990). Kriging: a method of interpolation for geographical information systems. International Journal of Geographical Information System, vol. 4(3), pp. 313-332.

Prashker, J. N., & Bekhor, S. (2004). Route choice models used in the stochastic user equilibrium problem: a review. Transport reviews, vol. 24(4), pp. 437-463.

Ramming, M. S. (2001). Network knowledge and route choice. Unpublished Ph. D. Thesis, Massachusetts Institute of Technology.

Raveau, S., Muñoz, J. C., & De Grange, L. (2011). A topological route choice model for metro. Transportation Research Part A: Policy and Practice, vol. 45(2), pp. 138-147.

Rust, J. (1994). Structural Estimation of Markov Decision Processes. Handbook of Econometrics, Chapter 4, pp. 3081-3143.

Ryan, S., & Frank, L. F. (2009). Pedestrian environments and transit ridership. Journal of Public Transportation, vol. 12(1), pp. 39-57.

Saberi, M., Aghabayk, K., & Sobhani, A. (2015). Spatial fluctuations of pedestrian velocities in bidirectional streams: Exploring the effects of self-organization. Physica A: Statistical Mechanics and its Applications, vol. 434, pp. 120-128.

Schüssler, N., & Axhausen, K. W. (2008). Identifying trips and activities and their characteristics from GPS raw data without further information. Arbeitsberichte Verkehrs-und Raumplanung, vol. 502.

Sevtsuk, A., & Basu, R. (2022). The role of turns in pedestrian route choice: a clarification. Journal of transport geography, vol. 102, 103392.

Sevtsuk, A., Basu, R., Li, X., & Kalvo, R. (2021). A big data approach to understanding pedestrian route choice preferences: Evidence from San Francisco. Travel Behaviour and Society, vol. 25, pp. 41-51.

Shahhoseini, Z., Sarvi, M., & Saberi, M. (2018). Pedestrian crowd dynamics in merging sections: Revisiting the "faster-is-slower" phenomenon. Physica A: Statistical Mechanics and its Applications, vol. 491, pp. 101-111.

Singleton, P. A. (2019). Walking (and cycling) to well-being: Modal and other determinants of subjective well-being during the commute. Travel behaviour and society, vol. 16, pp. 249-261.

Singleton, P. A., Park, K., & Lee, D. H. (2021). Varying influences of the built environment on daily and hourly pedestrian crossing volumes at signalized intersections estimated from traffic signal controller event data. Journal of transport geography, vol. 93, 103067.

Sun, B., & Park, B. B. (2017). Route choice modeling with support vector machine. Transportation research procedia, vol. 25, pp. 1806-1814.

Tal, G., & Handy, S. (2012). Measuring nonmotorized accessibility and connectivity in a robust pedestrian network. Transportation Research Record, vol. 2299(1), pp. 48-56.

The University of Hawaii at Manoa and Nelson Nygaard. (2012) The Campus Travel Demand Management Plan.

Vovsha, P., & Bekhor, S. (1998). Link-nested logit model of route choice: overcoming route overlapping problem. Transportation research record, vol. 1645(1), pp. 133-142.

Wang, Z., Novack, T., Yan, Y., & Zipf, A. (2020). Quiet route planning for pedestrians in traffic noise polluted environments. IEEE Transactions on Intelligent Transportation Systems, vol. 22(12), pp. 7573-7584.

Wu, T., & Li, Y. (2013). Spatial interpolation of temperature in the United States using residual kriging. Applied Geography, vol. 44, pp. 112-120.

Yang, F., Yao, Z., & Jin, P. J. (2015). GPS and acceleration data in multimode trip data recognition based on wavelet transform modulus maximum algorithm. Transportation Research Record, vol. 2526(1), pp. 90-98.

Yao, R., & Bekhor, S. (2022). A variational autoencoder approach for choice set generation and implicit perception of alternatives in choice modeling. Transportation Research Part B: Methodological, vol. 158, pp. 273-294.

Yao, R., & Bekhor, S. (2020). Data-driven choice set generation and estimation of route choice models. Transportation Research Part C: Emerging Technologies, vol. 121.

Zanlungo, F., Feliciani, C., Yücel, Z., Jia, X., Nishinari, K., & Kanda, T. (2023). A pure number to assess "congestion" in pedestrian crowds. Transportation Research Part C: Emerging Technologies, vol. 148.

Zhang, W., Buehler, R., Broaddus, A., & Sweeney, T. (2021). What type of infrastructures do e-scooter riders prefer? A route choice model. Transportation research part D: transport and environment, 94, 102761.

Zhang, X. S., Li, W., & Ouyang, Y. (2021). Paved guideway topology optimization for pedestrian traffic under Nash equilibrium. Structural and Multidisciplinary Optimization, vol. 63, pp. 1405-1426.

Zhou, B., Zheng, T., Huang, J., Zhang, Y., Tu, W., Li, Q., & Deng, M. (2020). A pedestrian network construction system based on crowdsourced walking trajectories. IEEE Internet of Things Journal, vol. 8(9), pp. 7203-7213.

Zimmermann, M., & Frejinger, E. (2020). A tutorial on recursive models for analyzing and predicting path choice behavior. EURO Journal on Transportation and Logistics, vol. 9(2).

Zimmermann, M., Mai, T., & Frejinger, E. (2017). Bike route choice modeling using GPS data without choice sets of paths. Transportation Research Part C: Emerging Technologies, vol. 75, pp. 183-196.